2008

Nitrated alpha-synuclein-activated microglial profiling for Parkinson's disease

Ashley D. Reynolds
University of Nebraska Medical Center, Omaha

Jason G. Glanzer
University of Nebraska Medical Center, Omaha, jglanzer@unmc.edu

Irena Kadiu
University of Nebraska Medical Center, Omaha, ikadiu@unmc.edu

Mary Ricardo-Dukelow
University of Nebraska Medical Center, Omaha

Anathbandhu Chaudhuri
University of Nebraska Medical Center, Omaha, achaudhuri@unmc.edu

See next page for additional authors

Published in *Journal of Neurochemistry* 104:6 (2008), pp. 1504-1525; doi 0.1111/j.1471-4159.2007.05087.x

Submitted August 21, 2007; revised manuscript submitted October 18, 2007; accepted October 18, 2007; published online October 24, 2007.

Nitrated alpha-synuclein-activated microglial profiling for Parkinson's disease

Ashley D. Reynolds,[1,2] Jason G. Glanzer,[1,2,7] Irena Kadiu,[1,2] Mary Ricardo-Dukelow,[1,2,3,8] Anathbandhu Chaudhuri,[1,2] Pawel Ciborowski,[1,4] Ronald Cerny,[5] Benjamin Gelman,[6] Mark P. Thomas,[1,2,9] R. Lee Mosley,[1,2] and Howard E. Gendelman,[1,2,3]

1 Center for Neurovirology and Neurodegenerative Disorders, University of Nebraska Medical Center, Omaha, Nebraska, USA
2 Department of Pharmacology and Experimental Neuroscience, University of Nebraska Medical Center, Omaha, Nebraska, USA
3 Department of Internal Medicine, University of Nebraska Medical Center, Omaha, Nebraska, USA
4 Department of Biochemistry and Molecular Biology, University of Nebraska Medical Center, Omaha, Nebraska, USA
5 Department of Chemistry, University of Nebraska-Lincoln, Lincoln, Nebraska, USA
6 Department of Pathology, University of Texas Medical Branch, Galveston, Texas, USA
7 Present address — Department of Oral Biology, College of Dentistry, University of Nebraska Medical Center, Lincoln, NE 68583, USA.
8 Present address — Department of Medicine, John A. Burns School of Medicine, University of Hawaii, Honolulu, HI 96813, USA.
9 Present address — School of Biological Sciences, University of Northern Colorado, Greeley, CO 80639, USA.

A. D. Reynolds and J. G. Glanzer contributed equally and should both be considered first authors of this study.

Corresponding author — H. E. Gendelman, Center for Neurovirology and Neurodegenerative Disorders, University of Nebraska Medical Center, 985880 Nebraska Medical Center, Omaha, NE 68198-5880; email hegendel@unmc.edu

Abstract

Microglial neuroinflammatory processes play a primary role in dopaminergic neurodegeneration for Parkinson's disease (PD). This can occur, in part, by modulation of glial function following activation by soluble or insoluble modified alpha-synuclein (α-syn), a chief component of Lewy bodies that is released from affected dopaminergic neurons. α-Syn is nitrated during oxidative stress responses and in its aggregated form, induces inflammatory microglial functions. Elucidation of these microglial function changes in PD could lead to new insights into disease mechanisms. To this end, PD-associated inflammation was modeled by stimulation of microglia with aggregated and nitrated α-syn. These activated microglia were ameboid in morphology and elicited dopaminergic neurotoxicity. A profile of nitrated, aggregated α-syn-stimulated microglia was generated using combinations of genomic (microarrays) and proteomic (liquid chromatography-tandem mass spectrometry, differential gel electrophoresis, and protein array) assays. Genomic studies revealed a substantive role for nuclear factor-kappa B transcriptional activation. Qualitative changes in the microglial proteome showed robust increases in inflammatory, redox, enzyme, and cytoskeletal proteins supporting the genomic tests. Autopsy brain tissue acquired from substantia nigra and basal ganglia of PD patients demonstrated that parallel nuclear factor-kappa B-related inflammatory processes were, in part, active during human disease. Taken together, the transcriptome and proteome of nitrated α-syn activated microglia, shown herein, provide new potential insights into disease mechanisms.

Keywords: alpha-synuclein, microglia, neuroinflammation, Parkinson's disease, proteomics

Abbreviations used: ACN, acetonitrile; AD, Alzheimer's disease; AFM, atomic force microscopy; BG, basal ganglia; DIGE, differential gel electrophoresis; DMEM, Dulbecco's modified Eagle's medium; ex/em, excitation/emission; FBS, fetal bovine serum; Gapdh, glyceraldehyde-3-phosphate dehydrogenase; IP, Immunoprecipitates; LB, Lewy bodies; LC-MS/MS, liquid chromatography-tandem mass spectrometry; LPS, lipopolysaccharide; NF-κB, nuclear factor-kappa B; N-α-syn, nitrated alpha synuclein; PBS, phosphate-buffered saline; PD, Parkinson's disease; PVDF, polyvinylidene fluoride; RIPA, radioimmunoprecipitation; ROS, reactive oxygen species; SN, substantia nigra; SNpc, substantia nigra pars compacta; TH, tyrosine hydroxylase; α-syn, alpha-synuclein.

Parkinson's disease (PD) is a progressive neurodegenerative disorder characterized by resting tremor, rigidity, bradykinesia, and gait disturbances (Fahn *et al.* 1998; Mayeux 2003; Fahn and Sulzer 2004). Presently, 1.5 million Americans are afflicted. Disease incidence rises with increasing age, with 120/100 000 contracting PD over the age of 70 (Dauer and Przedborski 2003). Pathologically, PD is characterized by the progressive loss of dopaminergic neuronal cell bodies in the substantia nigra pars compacta (SNpc) and their termini in the dorsal striatum (Hornykiewicz and Kish 1987). These pathological findings commonly parallel microglial activation observed in association with deposits of aggregated alpha synuclein (α-syn) in intracellular inclusions, known as Lewy bodies (LB) (Spillantini *et al.* 1997; Croisier *et al.* 2005). Although host genetics and environmental factors affect the onset and progression of PD (Tanner 1992) significant clinical, epidemiologic, and experimental data also support a role for microglial inflammation in disease pathogenesis (Forno *et al.* 1992; Banati and Blunt 1998;McGeer and McGeer 1998; Mirza *et al.* 2000;Cicchetti *et al.* 2002; Block and Hong 2005; Hong 2005; Wang *et al.* 2005).

The mechanisms underlying microglial activation in PD and how it affects neuronal survival is incompletely understood. One line of investigation is that neuronal death itself drives microglial immune responses (Giasson *et al.* 2000; Przedborski *et al.* 2001; Mandel *et al.* 2005). Alternatively, we, as well as others, have proposed that activation occurs as a consequence of release of aggregated proteins from the cytosol or within LB to the extracellular space. In this way, the death of dopaminergic neurons leads to release of modified protein aggregates that activate microglia inciting a lethal cascade of neuroinflammation and neuronal demise (Zhang *et al.* 2005; Wersinger and Sidhu 2006). Several lines of experimental evidence support this contention (Spillantini *et al.* 1997; Goedert 1999; Giasson *et al.* 2000; Kakimura *et al.* 2001; Croisier *et al.* 2005; Lee *et al.* 2005). *First*, aberrant expression of α-syn and PD pathogenesis are linked. This is derived from the discovery that mutations and multiple copies of the gene encoding α-syn (*SNCA* and *PARK1*) are linked to familial early onset PD (Kruger *et al.* 1998; Spira *et al.* 2001; Zarranz *et al.* 2004; (Singleton *et al.* 2003; Chartier-Harlin *et al.* 2004). *Second*, oxidation and nitration of α-syn leads to formation of aggregates and filaments that comprise LB (Giasson *et al.* 2000; Souza *et al.* 2000). *Third*, portions of α-syn are secreted rendering it more vulnerable to aggregation (Lee *et al.* 2005) and oxidative modification (Kakimura *et al.* 2001). *Fourth*, α-syn itself can activate microglia, inducing reactive oxygen species (ROS) (Thomas *et al.* 2007) and subsequent neurotoxicity (Zhang *et al.* 2005). *Fifth*, microglial products including cytokines, chemokines, excitotoxins, and proteins of the classical complement cascade affect a broad range of neurological diseases (McGeer and McGeer 1998; Bal-Price and Brown 2001; Liu and Hong 2003; Block and Hong 2005). *Sixth*, endogenous activators of microglia show a neuroinflammatory fingerprint reflective of what can occur during PD (Zhou *et al.* 2005; McLaughlin *et al.* 2006). *Lastly*, attenuation of microglial activation can protect up to 90% of dopaminergic neurons in PD animal models (Du *et al.* 2001; Teismann and Ferger 2001; Wu *et al.* 2002; Teismann *et al.* 2003; Kurkowska-Jastrzebska *et al.* 2004; Choi *et al.* 2005; Vijitruth *et al.* 2006).

Based on these observations, we investigated changes in the microglial transcriptome and proteome as a consequence of the cells' engagement with nitrated and aggregated α-syn (N-α-syn). N-α-syn stimulation of microglia induced morphological cell transformation and neurotoxic secretions. A N-α-syn-activated 'microglial signature' was determined by gene microarrays, 2D differential in-gel electrophoresis (DIGE), and by cytokine profiling. N-α-syn induced a microglia inflammatory phenotype characterized by the expression of neurotoxic and neuroregulatory factors. Most importantly, the inflammatory signature seen in laboratory assays were, in part, mirrored in parallel tests performed on postmortem brain tissues from PD patients. These observations, taken together, serve to support both a 'putative' role for N-α-syn-activated microglia in disease.

Materials and methods

Parkinson's disease brain tissues

Autopsy materials from the substantia nigra (SN) and basal ganglia (BG; caudate nucleus and putamen) of 10 patients who died with signs and symptoms of PD, three with Alzheimer's disease (AD), and 10 age-matched controls were secured from the National Research Brain Bank Tissue Consortium. The 10 controls ranged in age from 62 to 91 and died of diseases unrelated to neurological impairments. This included atherosclerotic and metabolic diseases, infections, and cancer (Table 1).

An antibody to N-α/β-syn (clone nSyn12, mouse ascites; Upstate, Charlottesville, VA, USA) that recognizes nitrated human N-α-syn (14.5 kDa) and N-β-syn (17 kDa) was used for immunoprecipitation. Samples of SN from control, AD, and PD autopsy brain tissues (Table 1) were homogenized in ice-cold radioimmunoprecipitation (RIPA) buffer, pH 7.4 and centrifuged at 10 000 g for 10 min at 4°C to remove cellular debris. Protein A/G PLUS-agarose beads (Santa Cruz Biotechnology Inc., Santa Cruz, CA, USA) were added to 1 mg total cellular protein and incubated for 30 min at 4°C. Beads were pelleted by centrifugation at 1000 g for 5 min at 4°C. The supernatants were incubated overnight at 4°C with 2 μg of primary antibody, then with Protein A/G PLUS-agarose beads for 6 h on a rotating device at 4°C. Immunoprecipitates (IP) were collected after centrifugation at 1000 g for 5 min at 4°C, washed with phosphate-buffered saline (PBS), and resuspended in 20 μL of 1× electrophoresis sample buffer.

Nitrated-α-Syn IP (20 μL) were fractionated by 16% Tricine sodium dodecyl sulfate–polyacrylamide gel electropho-

Table 1. Patient clinical profiles and neuropathological findings[a]

Patient	Diagnosis[b]	Gender	Age[c]	Duration[d]	Neuropathology[e]
1	PD	Female	78	25	Hypopigmentation and LB formation in SN and locus ceruleus
2	PSP	Male	83	N/A	Cerebral atrophy of frontal and superior temporal
3	PD	Female	75	9	Idiopathic
4	PD	Female	89	21	Idiopathic
5	PD	Female	82	10	Neocortical LB
6	LBD	Male	82	8	Neocortical LB and hippocampal sclerosis
7	PSP	Male	82	24	Degeneration of subcortical nuclei with neurofibrillary tangles
8	PD	Male	67	17	Hypopigmentation, neuronal loss, gliosis, LB in SN, and locus ceruleus
9	PD	Female	85	3	Hypopigmentation, gliosis, and neuronal loss in SN, globus pallidus, and caudate-putamen
10	PD	Male	86	5	Hypopigmentation, LB, neuronal loss in the SN and locus ceruleus
11	AD	Male	73	8	Neuritic and diffuse plaques and neurofibrillary tangles in neocortex and hippocampus. Neuronal loss in Locus ceruleus.
12	AD	Female	84	N/A	Remote infarct in the occipital lobe and cerebellum
13	AD	Male	76	N/A	Senile plaque-predominant AD

[a] Ten non-affected, age-matched controls were used for comparisons in this study; [b] Final diagnosis at autopsy; [c] Age at death; [d] Duration of disease (years) based on onset of initial symptoms and preliminary diagnosis; [e] Neuropathology at autopsy.

PD, Parkinson's disease; PSP, progressive subnuclear palsy; LBD, Lewy body disease; LB, Lewy bodies; SN, substantia nigra; N/A, data not available; AD, Alzheimer's disease; N/A, data not available.

resis (PAGE) (Jule Inc., Milford, CT, USA and BIORAD Laboratories Inc., Los Angeles, CA, USA) at constant voltage for 1.5 h. The gels were fixed and stained with Coomasie Blue to visualize protein bands. Bands corresponding to the molecular weights encompassing 14.5 kDa (α-syn) were excised, digested by trypsin, column purified, and sequenced by liquid chromatography-tandem mass spectrometry (LC-MS/MS) for protein validation. Sequenced peptides were distinguished by peptide matches to the human α-syn sequence (NCBI Accession: AAI08276).

Purification, nitration, and aggregation of recombinant mouse α-syn

Purification, nitration, and aggregation of recombinant mouse α-syn were performed as previously described (Thomas *et al.* 2007). Five individual lots of α-syn were tested for endotoxin by Limulus amebocyte lysate tests and all were below the limit of detection for endotoxin (< 0.05 endotoxin units). Amino acid analysis to determine protein concentration using HPLC was performed by the University of Nebraska Medical Center Protein Structure Core Facility. Proteins were separated by PAGE using 4–12% NuPAGE gels (Invitrogen, Carlsbad, CA, USA). After electrophoresis, the gels were transferred onto polyvinylidene fluoride (PVDF) membranes (Millipore, Billerica, MA, USA) and probed with primary mouse IgG1 anti-α-syn (1 : 500; Transduction Laboratories/BD Biosciences, Franklin Lakes, NJ, USA) or primary rabbit IgG anti-nitrotyrosine (1 : 2000; Upstate). Signal was detected with horseradish peroxidase-conjugated anti-mouse IgG or anti-rabbit IgG (both from Zymed Laboratories, South San Francisco, CA, USA) using chemiluminescence systems (SuperSignal® West Pico Chemiluminescent Substrate; Pierce Biotechnology Inc., Rockford, IL, USA). For visualization of the protein by atomic force microscopy (AFM), samples were deposited on mica, glued to a glass slide, and dried under argon gas flow. The image was taken in air, height, amplitude, and phase modes using a Molecular Force Probe 3D controller (Asylum Research Inc., Santa Barbara, CA, USA).

Isolation, cultivation, and N-α-syn activation of murine microglia

Microglia from C57BL/6 mice neonates (1- to-2-days old) were prepared according to well described techniques (Dobrenis 1998). All animal procedures were in accordance with National Institutes of Health guidelines and were approved by the Institutional Animal Care and Use Committee of the University of Nebraska Medical Center. Brains were removed and placed in Hanks' Balanced Salt Solution at 4°C. The mixed glial cells were cultured for 7 days in Dulbecco's Modified Eagle's Medium (DMEM) containing 10% fetal bovine serum (FBS), 10 μg/mL gentamicin, and 2 μg/mL macrophage colony stimulating factor (a generous gift of Wyeth Inc., Cambridge, MA, USA). To obtain homogenous microglial cell populations, culture flasks were gently shaken and non-adherent microglia were transferred to new flasks. The flasks were incubated for 30 min to allow the microglia to adhere, and loose cells removed by washing with DMEM. Microglia were plated at 2×10^6 cells per well in six-well plates in DMEM containing 10% FBS, 10 μg/mL gentamicin, and 2 μg/mL macrophage colony stimulating factor. One week later, cells were stimulated with 100 nmol/L of aggregated N-α-syn/well or no stimulation for 4 h. Media were replaced with serum-free DMEM without phenol red or other additives (Invitrogen) and incubated for 24 h in a 37°C, 5% CO_2 incubator.

Inflammatory genomic and PCR assays

RNA from N-α-syn stimulated primary murine microglial cells and unstimulated control was extracted with TRIzol (Invitrogen), column purified (Qiagen, Valencia, CA, USA), precipitated with ammonium acetate, amplified and labeled using the T7-based TrueLabeling-AMP 2.0 kit (Superarray, Frederick, MD, USA). The resultant cRNA was hybridized to an oligo-

based microarray for mouse general pathway (Superarray #OMM-014) and nuclear factor-kappa B (NF-κB)-related genes (Superarray #OMM-025). The arrays were washed, incubated sequentially with streptavidin-bound alkaline phosphatase and chemiluminescent substrate before exposure to X-ray film. Subsequent analysis of the microarrays was performed using the GEArray expression analysis suite (Superarray).

Total RNA obtained from analysis of the microglial transcriptome was reverse transcribed with random hexamers and SSII reverse transcriptase (Applied Biosystems, Foster City, CA, USA). Murine-specific primer pairs were: *Ccl2*: CCCCAAGAAGGAATGGGTCC and GGTTGTGGAAAAGGTAGTGG; *Il1β*: GTTCCTTTGTGGCACTTGGT and CTATGCTGCCTGCTCTTACTGACT; *Il10*: CAGTTATTGTCTTCCCGGCTGTA and CTATGCTGCCTGCTCTTACTGACT; *Ifng*: TTTGAGGTCAACAACAACCCACA and CGCAATCACAGTCTTGGCTA; and *Nos2*: 5′-GGCAGCCTGTGAGACCTTTG-3′ and 5′-GAAGCGTTTCGGGATCTGAA-3′. TaqMan gene expression assays specific for murine *Tnf*, *Tnfrsf1a*, *Stat1*, *Rela*, *Bdnf*, and *Gdnf* were purchased from Applied Biosystems, and normalized to glyceraldehyde-3-phosphate dehydrogenase (*Gapdh*) expression. Tissue samples obtained from PD and control patients were snap frozen on dry ice and stored at −80°C. RNA was prepared from the samples using TRIzol reagent (Invitrogen) and purified with the RNeasy Mini Kit (Qiagen), prior to cDNA synthesis. Human specific primers for *TNF*, *TNFRSF1A*, *STAT1*, *NFKB1*, *RELA*, *BDNF*, and *GDNF* were analyzed using TaqMan gene expression assays. Gene expression was normalized to the housekeeping gene *Gapdh*. Real-time quantitative PCR was performed with cDNA using an ABI PRISM 7000 sequence detector (Applied Biosystems). Reverse SYBR Green I detection system was used, and the reactions generated a melting temperature dissociation curve enabling quantitation of the PCR products.

Cytokine arrays

Microglia were plated at a density of 2×10^6 cells/well in a six-well plate and stimulated with 100 nmol/L aggregated N-α-syn, and 100 ng/mL lipopolysaccharide (LPS, *Escherichia coli*; Sigma-Aldrich, St. Louis, MO, USA) in serum-free media. Fifty microliter aliquots were collected at 8, 24, and 72 h of incubation in triplicate and frozen at −80°C. For assay, the samples were analyzed using the BD Cytometric Bead Array Mouse Inflammation Kit (BD Biosciences, San Jose, CA, USA) according to the manufacturer's protocol. Samples of culture supernatants from microglia were diluted 1 : 3 and 1 : 10 in assay diluent and analyzed for cytokine concentration with a FACSCalibur flow cytometer (BD Biosciences). Concentrations of cytokines were determined from a standard curve created with serial dilutions of the cytokine standards provided by the manufacturer.

Neurotoxicity assays

MES23.5 cells, kindly provided by Dr Stanley Appel, were cultured in 75-cm^2 flasks in DMEM/F12 with 15 mmol/L HEPES (Invitrogen) containing N2 supplement (Invitrogen), 100 U/mL of penicillin, 100 μg/mL streptomycin, and 5% FBS. Cells were grown to 80% confluence then co-cultured at 1 : 1 ratio with previously plated microglial cells. To assess cell viability microglia cells were plated at a density of 5×10^4 cells on sterile glass coverslips, and co-cultures were prepared with a 1 : 1 ratio microglia: MES23.5 cells. After 24–48 h, cells were stimulated with aggregated 100 nmol/L N-α-syn or 100 nmol/L α-syn for 4, 8, 24, and 72 h. $CD11b^+$ microglial cells were distinguished from MES23.5 cells by APC-conjugated CD11b (1 : 200; Invitrogen) immunocytochemistry. For tyrosine hydroxylase (TH) cytostaining, cells were fixed in 4%p-formaldeyde, permeablized, and blocked in 2% normal goat serum with 0.25% Triton X-100 in PBS for 30 min, and probed with rabbit polyclonal anti-TH (1 : 1000; EMD Biosciences Inc., San Diego, CA, USA), followed by FITC goat anti-rabbit IgG. For western blot analysis, 10 μg of protein sample from cell lysates of each treatment group was loaded onto a 12% NuPAGE Bis–Tris gel (Invitrogen). Following transfer onto a PVDF membrane, the membrane was blocked and then probed overnight with anti-TH (1 : 1000). Signal was detected with horseradish peroxidase-conjugated anti-rabbit IgG (1 : 10 000; Zymed Laboratories) using chemiluminescence system (SuperSignal® West Pico Chemiluminescent substrate; Pierce Biotechnology Inc.). Densitometric analysis was performed using ImageJ software and normalized to β-actin (1 : 1000; Abcam, Cambridge, MA, USA). Assays for viable and dead mammalian cells (Live/Dead Viability/Cytotoxicity; Invitrogen) were performed according to manufacturer's protocol. The protocol was revised so that the concentration of each dye was 1 μmol/L to avoid high background. Live cells were distinguished by the uptake of calcein acetoxymethyl ester to acquire a green fluorescence [excitation/emission (ex/em) 495/515 nm], while dead cells acquired a red fluorescence (ex/em 495/635 nm) because of the uptake of ethidium homodimer-1. Cell enumerations were performed using fluorescence microscopy (200× magnification) and a M5 microplate fluorometer (Molecular Devices, Sunnyvale, CA, USA) (Limit 1 ex/em 490/522 nm and Limit 2 ex/em 530/645 nm). The number of viable MES23.5 cells in each treatment group was normalized as the percentage of surviving cells in unstimulated culture controls.

Protein purification, 2D DIGE, and DeCyder analyses

Cell lysates of microglia were prepared with 5 mmol/L Tris–HCl, pH 8.0, 1% 3-[(3-cholamidopropyl)-dimethylammonio]-1-propane sulfonate and a cocktail of protease inhibitors (Sigma-Aldrich). Protein content was quantitated using a DC Protein Assay (BioRad, Hercules, CA, USA). Factors known to interfere with isoelectric focusing (first dimension separation in 2D sodium dodecyl sulfate–PAGE) such as salts and detergents were removed from cell lysates using the 2D Cleanup kit (GE Healthcare, Piscataway, NJ, USA) according to manufacturer's protocol. Protein concentration was determined using 2D Quant (GE Healthcare). Samples of control and stimulated cell lysates (25 μg of each lysate) were labeled with 400 pmol of CyDye 2. A 50 μg protein sample of control cell lysate was labeled with 400 pmol of CyDye 3; and a 50 μg protein sample of stimulated cell lysate was labeled with 400 pmol of CyDye 5. Labeling was performed following the manufacturer's protocols. The samples were pooled, resuspended in rehydration buffer to a total volume of 450 μL, then loaded onto an immobilized pH gradient strip, and left for 18 h for rehydration. In the first dimension, samples were run in IPGphor and in Ettan DALTsix electrophoresis apparatus (GE Healthcare) for the second dimension. CyDye 3- and CyDye 5-derivatized proteins were detected in gels using a Typhoon 9400 Variable Mode Imager with ex–em filters at 540/590 nm for CyDye 3 dyes and 620/680 nm for CyDye 5 dyes (GE Healthcare). Analysis of CyDye 3-CyDye 5 image pairs, adjustment to CyDye 2 control im-

ages, and detection of protein spots with relative spot volumes were performed using DeCyder software (GE Healthcare) to locate and analyze multiplexed samples within the gel. Selected protein spots of interest were excised from the 2D gel using an Ettan Spot Picker. The proteins from gel pieces were digested with trypsin, as described below, and resultant peptides were analyzed using LC-MS/MS system (ThermoElectron Inc., Waltham, MA, USA). Protein identification was completed using BIOWORKS 3.1 software.

In gel tryptic digestion and protein identification by LC-MS/MS

Specific protein spots were excised from the gels by an automated Ettan spot picker. Following column purification (ZipTip $_{CU-18}$; Millipore) with 50% acetonitrile (ACN), 50 mmol/L NH_4HCO_3/50% ACN, and 10 mmol/L NH_4HCO_3/50% ACN, gel pieces were dried and incubated with trypsin (100 ng/μL) (Promega, Sunnyvale, CA, USA) for 12–18 h. Samples were extracted by 0.1% trifluoroacetic acid/60% ACN, pooled, and dried.

Dried peptide samples were reconstituted in 0.1% formic acid/HPLC-grade water, detected on a ProteomeX LCQ™ DECA XP Plus mass spectrometer (ThermoElectron Inc.), and identified using BioWorks 3.1SR software. Proteins identified by peptides having a Unified Score (BioWorks 3.1SR, ThermoElectron Inc.) greater than 3000 were marked for further analysis.

Nuclear/cytosol fractionation

Cell lysates were prepared from SN of PD and control patients by homogenization in PBS. Cells were collected following centrifugation at 500 g for 5 min. Cytosol and nuclear fractions were prepared using the Nuclear/Cytosol Fractionation Kit (BioVision, Mountain View, CA, USA) according to manufacturer's protocol.

Western blot assays

Protein was prepared from cell lysates in RIPA buffer supplemented with protease inhibitors (Pierce Biotechnology Inc.). Protease inhibitor cocktail was added to each conditioned media sample fraction prior to processing. Following centrifugation at 10 000 g for 10 min, the supernatants were removed and allowed to dialyze against water overnight. Tissue samples obtained from PD and control patients were snap frozen on dry ice and stored at −80°C. Protein lysates were prepared from individual samples through homogenization in RIPA buffer supplemented with protease inhibitors (Pierce Biotechnology Inc.). Protein quantification was performed using the bicinchoninic acid kit (Pierce Biotechnology Inc.). Protein concentration of each sample was determined using a calibration curve generated from purified bovine serum albumin. A total of 20 μg of each sample was loaded onto 4–12% Bis–Tris NuPAGE gels (Invitrogen) and transferred onto PVDF membranes (BioRad). Primary antibodies to calmodulin (1 : 1000) and 14-3-3σ (1 : 200) (Millipore), biliverdin reductase (1 : 5000), thioredoxin (1 : 2000), β-actin (1 : 5000), and α-tubulin (1 : 5000) purchased from Abcam, L-plastin (1 : 1000), α-enolase (1 : 1000), glutathione-*S*-transferase (1 : 1000), and NF-κB p65 and p50 (1 : 200) purchased from Santa Cruz Biotechnology Inc. were used for analyses. Blots were probed with the respective horseradish peroxidase-conjugated secondary antibodies (1 : 5000; Invitrogen) and detected using SuperSignal West Pico Chemiluminescent substrate (Pierce Biotechnology Inc.). The intensity of protein bands was quantified using IMAGEJ and normalized to Gapdh (1 : 5000; Santa Cruz Biotechnology Inc.) level in the same sample.

Statistical analyses

All values are expressed as mean ± SEM. Differences among means were analyzed by Student's *t*-test or by one-way ANOVA followed by Bonferroni *post hoc* testing for pair-wise comparison.

Results

Aggregated N-α-syn and microglial activation: laboratory and pathological studies

To investigate the mechanisms by which N-α-syn-mediated microglial activation affects dopaminergic neurodegeneration, we created a cellular model that would reflect the salient features of neuroinflammation as it could occur in PD. To this end, we first determined if N-α-syn was present in regions of brain where microglial activation is known to be present in PD. Whole cell lysates consisted of several protein bands following gel electrophoresis (data not shown) and Coomassie staining (data not shown). IP assays performed from SN tissues of PD patients using a primary antibody against nitrated α/β-synulcein showed a greater than twofold increase in intensity of the protein band corresponding to 14–14.5 kDa ($p < 0.001$) than that present in control patients (Figure 1a) or in patients diagnosed with AD (data not shown) along with higher molecular weight species greater than 17 kDa (data not shown). Peptide sequence analyses by LC-MS/MS revealed that the protein band encompassing the 14–14.5 kDa of the anti-N-α-syn IP contained peptides with sequence homology to human α-syn in SN samples recovered from PD brains (Figure 1a, highlighted sequences). Interestingly, such sequence homologies to α-syn were not identified from 14 to 14.5 kDa proteins in either control or AD samples. Thus, we next sought to develop an *in vitro* model to reflect conditions present in an affected human host, but using the murine analog. Here, recombinant mouse α-syn was purified, nitrated, and aggregated for use as a microglial stimulant. Western blot assays showed cross-linking of N-α-syn monomers (Souza *et al.* 2000) and higher molecular weight aggregates, thus verifying the nitration and aggregation of α-syn (Figure 1b). The aggregated N-α-syn contained a substantially reduced monomeric band (corresponding to a band at ~14 kDa) but higher molecular weight banding aggregates. Analysis of protein aggregation was also assessed by AFM. Samples of N-α-syn contained low numbers of globular aggregates (2–6 nm in height) prior to aggregation. However, following aggregation, N-α-syn was present predominately as oligomers (2–6 nm in height). In addition, there were few protofibrils (1.5–2.5 nm in height), filaments, and fibrils (~5–8 nm in height) present (Figure 1c). Non-nitrated α-syn was present in similar configurations (data not shown).

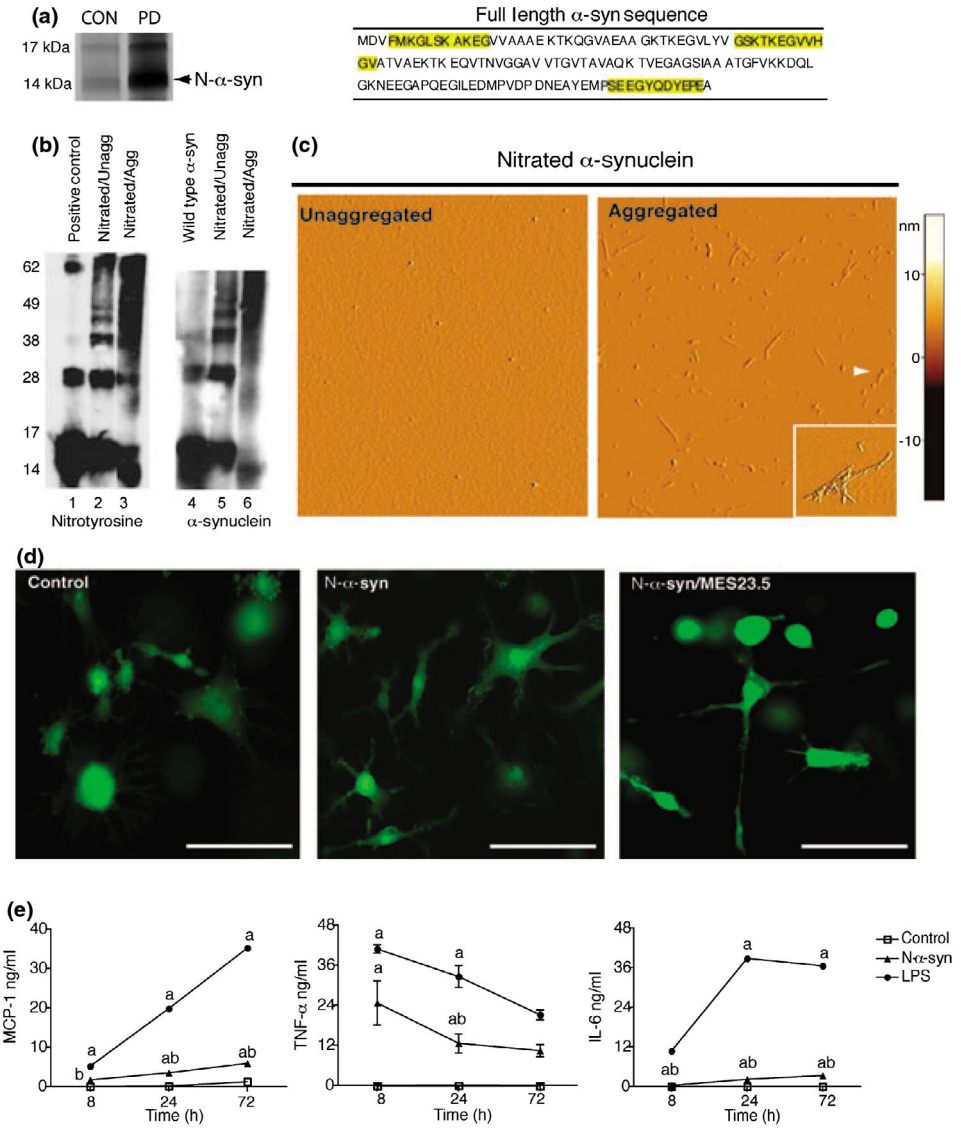

Figure 1. α-Syn nitration, aggregation, and microglial activation. **(a)** Coomassie stain of anti-N-α/β-synuclein immunoprecipitation from SN from control and PD brains. Arrowhead reflects the area excised from gel and submitted for LC-MS/MS analysis. Equal concentrations of proteins from control and experimental brain tissues served as loading controls. Peptides obtained by LC-MS/MS that matched human α-syn are highlighted within the full-length sequence. **(b)** Western blot analyses of recombinant mouse α-syn and derivatives. Lane 1 is a nitrotyrosine modified protein provided by the manufacturer. Lanes 1–3 were blotted and probed with anti-nitrotyrosine, and lanes 4–6 were probed with anti-synuclein. **(c)** AFM images are shown for unaggregated (0.4 × 0.4 mm) and aggregated N-α-syn (1.6 × 1.6 mm). Arrow indicates location of inset photomicrograph. Scale bar corresponds to height of aggregates on the interface. **(d)** Microglial morphology after exposure of microglia to media alone (control, left) or 100 nmol/L N-α-syn (center), and N-α-syn stimulated microglia in co-culture with MES23.5 cells (right; scale bar: 25 μm). Cells were stained with calcein AM to detect viable cells. **(e)** Cytokine bead arrays were used for flow cytometric analysis of supernatants from unstimulated microglia (control, open box) and microglia stimulated with either 100 nmol/L N-α-syn (closed triangle) or 100 ng LPS (closed circle) (n = 3, p < 0.01 vs. [a]Control and [b]LPS at each corresponding time point).

We next evaluated the stimulatory effects of N-α-syn on microglia. The dose of 100 nmol/L (14.5 ng protein/mL) was selected based on previous extensive works performed in our laboratories demonstrating that, following a dose-response of N-α-syn, 100 nmol/L (50% over control) is required to induce substantive ROS from activated microglial cells (Zhang *et al.* 2005; Thomas *et al.* 2007) as well as cytotoxicity. ROS production was slightly decreased in comparison with either 50 or 500 nmol/L of N-α-syn. While native α-syn is ubiquitously expressed, the physiological concentration of N-α-syn in disease has not been elucidated. However, based on concentrations of modified α-syn in affected PD brain tissues, 100 nmol/L concentration is at physiologically relevant levels (Hal-

liday *et al.* 2005) and is below that detectable by immunohistochemistry in neuronal inclusions within the SN of PD brains (≥ 100 ng). Phenotypic transformation into an ameboid morphology commonly follows microglial activation with different pro-inflammatory stimuli (Giulian *et al.* 1995; Vilhardt 2005). Thus, we examined if changes in microglial morphology would be elicited following N-α-syn activation. Resting microglia were both round and ellipsoid shaped with retracted processes that were characteristic of a relatively quiescent phenotype (Figure 1d). In contrast, N-α-syn activated microglia assumed a more ameboid appearance with extensive processes, characteristic, in part, of an activated phenotype. N-α-syn-stimulated microglia co-cultured with MES23.5 cells acquired a rod-like appearance and further extension of processes.

We recently demonstrated that 100 nmol/L of aggregated N-α-syn could activate microglia to produce copious amounts of ROS (Thomas *et al.* 2007). In contrast, unaggregated N-α-syn or minced neuronal membrane fractions failed to induce significant amounts of ROS above control levels. This suggested that the microglial response to N-α-syn was specific and could not be elicited in response to unaggregated protein or by phagocytosis under the same conditions. Therefore, we assessed the extent of the neuroinflammatory phenotype induced by N-α-syn stimulation of microglia. Quantification of common cytokines and chemokines that are secreted in response to inflammatory stimuli was performed by cytometric bead array. LPS-activated microglia served as a positive control. Stimulation with N-α-syn enhanced the secretion of TNF-α, IL-6, MCP-1 (Figure 1e), and IFN-γ (data not shown) compared with basal levels observed in unstimulated microglia. These results are consistent with the induction of an inflammatory microglial phenotype following N-α-syn stimulation. The parallels between N-α-syn and LPS-induced cellular effects support a commonality for innate immune responses in disease and suggest that these pro-inflammatory processes may be common among mononuclear phagocytes that recognize disparate activators.

N-α-syn-stimulated microglia are neurotoxic to MES23.5 dopaminergic cells

To determine the effect of N-α-syn-activated microglia on neuronal survival, the dopaminergic MES23.5 cell line was used as an indicator for cytotoxicity measurements by co-culture with stimulated and unstimulated microglia. MES23.5 cell death was determined by measuring immunoreactivity for the rate-limiting enzyme in dopamine synthesis, TH, expressed by MES23.5 cells, and the Live/Dead cell assay. During stimulation with 100 nmol/L N-α-syn, the number of TH+ cells declined in the stimulated cultures, resulting in a significant diminution in TH-immunoreactive cells (8 h: 74.6% of control; 24 h: 53.4% of control, $p < 0.01$; 72 h: 48.5% of control, $n = 6$, $p < 0.01$). Western blot analysis confirmed this observation, as TH expression decreased in a time-dependent manner over the course of N-α-syn stimulation (TH+/β-actin ratio at 8 h: 94.6% of control; 24 h: 86.2% of control; 72 h: 64.9% of control, $p < 0.01$). Analysis of cell viability with the Live/Dead cell assay demonstrated that stimulation of microglia with 100 nmol/L of N-α-syn followed by MES23.5 co-culture resulted in remarkable reduction of viable cells with concomitant increase in dead MES23.5 cells; whereas, fewer dead cells were observed in co-cultures with microglia stimulated with α-syn (non-nitrated) after 24 h (Figure 2a). Percentage of MES23.5 cell survival was less in co-cultures with microglia stimulated with α-syn (83%) and N-α-syn (58%) compared with unstimulated controls (95%) at 72 h (Figure 2b). The more sensitive fluorometric analysis revealed as early as 24 h after stimulation a similar pattern of progressive decline in viable cells in the presence of α-syn and N-α-syn stimulated microglia to 76% and 65% of controls at 24 h of stimulation, respectively (Figure 2c). Moreover, N-α-syn-mediated cytotoxicity was restricted to MES23.5 cells, as stimulation of microglia in the absence of MES23.5 cells neither affected microglial survival (Figure 2d) nor yielded a significant difference in the number of dead $CD11b^+$ cells between control and stimulated cultures (data not shown). In addition, cytotoxicity of MES23.5 cells was not elicited with N-α-syn in the absence of microglia (Figure 2d). Furthermore aggregation of N-α-syn was necessary for inducing microglia cytotoxicity (Figure 2d). Importantly, a decrease in the cell survival was observed when microglia were stimulated with either aggregated α-syn (93%) or N-α-syn (86%) for 24 h, and co-cultured with MES23.5 cells in transwell inserts, but not unaggregated protein. MES23.5 cultures incubated with supernatants obtained from microglia stimulated with either α-syn or N-α-syn resulted in decreased cell survival (89% and 84%, respectively) compared with supernatants from unstimulated microglia (Figure 2e).

NF-κB gene expression and nuclear translocation in PD

NF-κB pathway activation is critical for the initiation of inflammatory events including the production of inflammatory cytokines and chemokines linked to inflammation and microglial activation. We hypothesized that acquisition of such an inflammatory phenotype begins with induction of gene products that ultimately leads to neurotoxic factor production, cell migration, and apoptosis. To determine the extent to which this pathway was operative in PD, the SN and BG of PD brains (clinical and neuropathological profiles shown Table 1) and controls (those without neurological disease) were analyzed for NF-κB-related genes as well as neurotrophin expression (Figure 3). Increases, albeit modest, were seen in *NFKB1* expression from samples of SN from PD patients com-

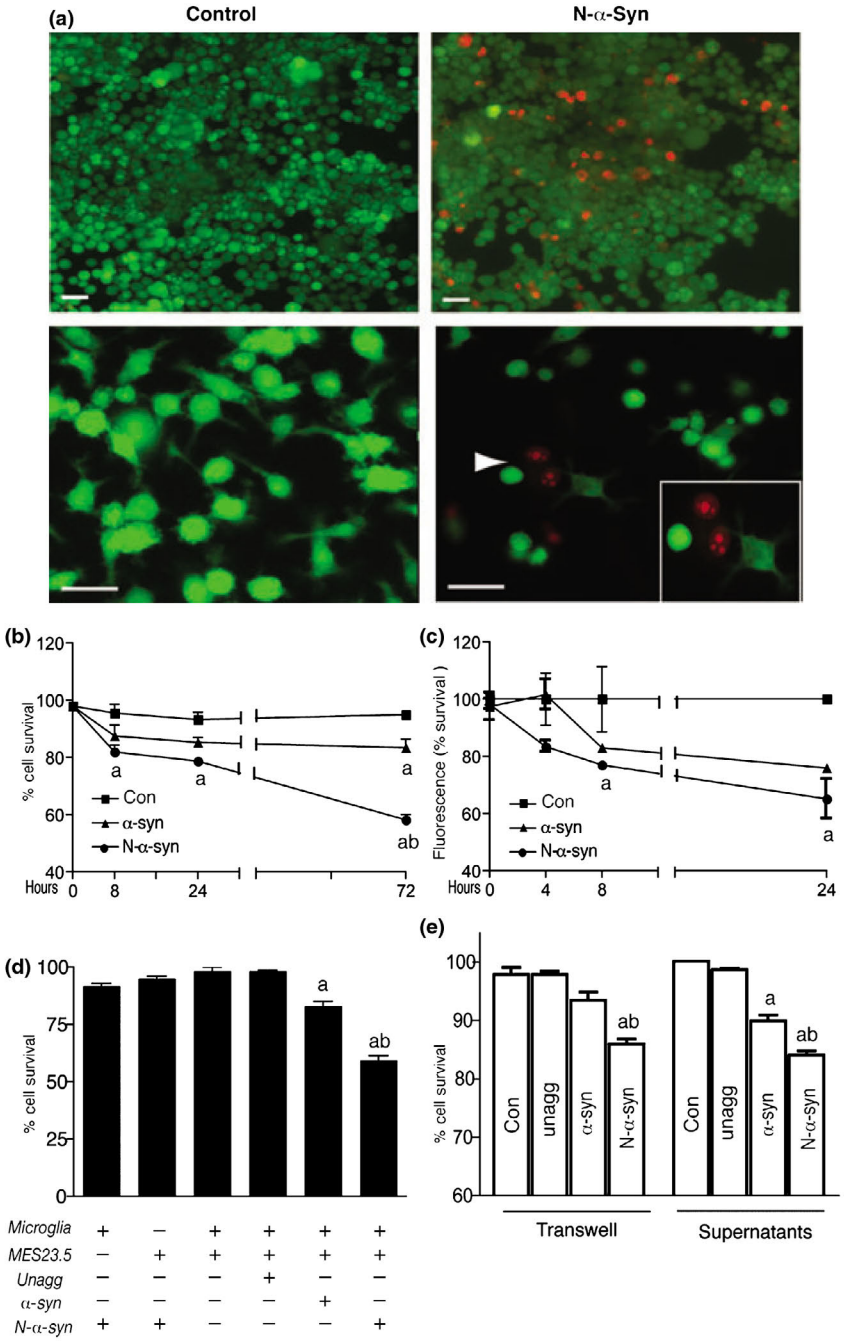

Figure 2. N-α-syn-stimulated microglia decrease dopaminergic cell survival. (**a**) Representative photomicrographs of Live/Dead assays of unstimulated or N-α-syn stimulated microglia co-cultured with MES23.5 cells for 24 h. Viable cells appear green and dead cells are red. (scale bars: 25 μm). (**b** and **c**) N-α-syn-induced microglial inhibition of cell survival. A time-course for cell survival is shown for MES23.5 cells and microglia co-cultured in the presence of media alone (Con, box), 100 nmol/L unmodified α-synuclein (α-syn, triangle), or 100 nmol/L N-α-synuclein (N-α-syn, circle). Cell viability was quantified using the Live/Dead assay by (**b**) cell count (n = 9 fields, $p < 0.01$ compared with [a]0 h and [b]all treatment groups at corresponding time point), and by (**c**) fluorometric analysis (n = 9 fields, $p < 0.01$ compared with [a]0 h and [b]all treatment groups at corresponding time point). (**d**) Cell survival of MES23.5 cells in co-culture with microglia after 72 h of stimulation with either α-syn or N-α-syn (n = 9, p < 0.01 compared with [a]all treatment groups and [b]α-syn stimulated microglia). (**e**) Influence of secretory factors from microglia stimulated with either α-syn or N-α-syn for 24 h on MES23.5 cells was determined. Cell survival was assessed following incubation with supernatants or in transwell format for 24 h (n = 3, $p < 0.01$ compared with [a]all treatment groups and [b]α-syn-stimulated microglia).

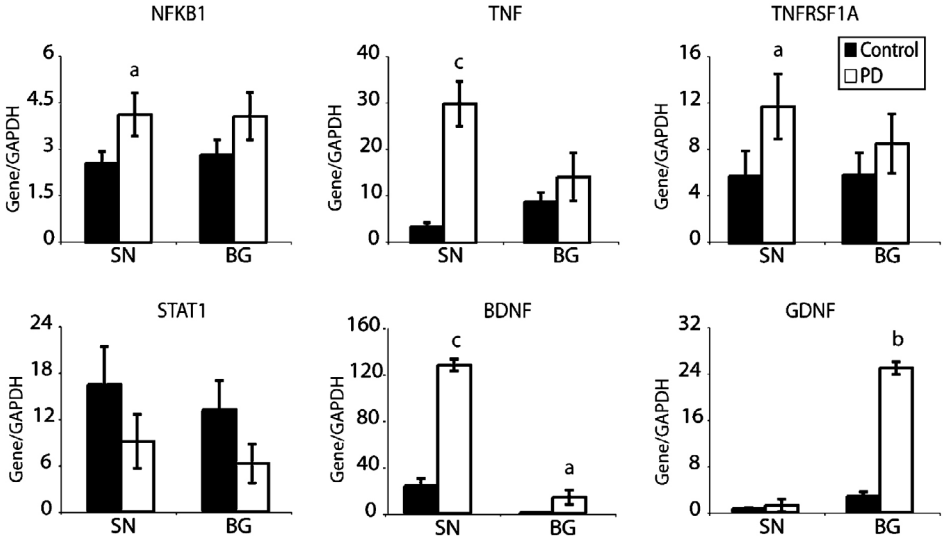

Figure 3. Cellular activation and oxidative stress pathways in PD brain tissues. Tissue samples from the SN and BG of control (filled bars) and PD patients (open bars) (Table 1) were evaluated by qRT-PCR for expression of NF-κB pathway associated genes. The relative expression of a gene was normalized to GAPDH in the same sample and values are represented as mean ± SEM ([a] $p < 0.05$, [b] $p < 0.01$, and [c] $p < 0.001$ compared with samples from control patients, $n = 8–10$ patients per group).

pared with controls; whereas, no significant difference was observed for *RELA* expression (data not shown). However, an eightfold increase in TNF expression was observed in the SN and BG together with a twofold increase in expression of its receptor *TNFRSF1A*. *STAT1* was minimally decreased in PD brains. Similarly, analysis of AD brain tissues as a control for neuroinflammatory pathology also revealed a moderate induction of NF-κB transcription factors *NFKB1* and *RELA*, while *TNF* expression was increased 40- and 10-fold in the SN and BG along with modest elevations of *STAT1* in AD brain tissues compared with controls (data not shown). Based on these findings, we reasoned that a compensatory trophic mechanism could be operative in PD. Indeed, *BDNF* was shown to be increased greater than sixfold in the SN and twofold in the BG in PD. Consistent with recent observations by others (Backman *et al.* 2006), *GDNF* was increased greater than 10-fold in the BG but no significant changes were observed in the SN.

A recent investigation by immunofluorescence analysis of midbrain sections revealed a marked increase in expression of NF-κB p65 in the SN of PD patients compared with controls, which co-localized to $CD11b^+$ microglia in addition to affected neurons (Ghosh *et al.* 2007). In the current study cytosolic and nuclear fractions were prepared from the lysates of SN of PD and control brain tissues, and lysates analyzed for NF-κB protein subunits p50 and p65. Increased expression of NF-κB subunits in both the cytosolic fractions and nuclear fractions were observed in PD brain tissues (Figure 4). Phosphorylation of serine 536 (pS536) critical for RelA/p65 transcriptional activity was also increased in PD brain tissues.

N-α-syn-activated microglia and the PD transcriptome are linked through NF-κB

The increased expression of NF-κB transcription identified in the SN of PD brains and the microglial response to N-α-syn stimulation that were consistent with inflammatory responses suggested that one major signaling pathway induced by N-α-syn involves NF-κB activation. Use of a general microarray confirmed that NF-κB expression was increased by stimulation with N-α-syn (Figure 5a). Using NF-κB-focused microarrays (Figure 5b, Table 2), we showed increased expression of genes encoding proinflammatory cytokines, including *Tnf*, *Ccl2*, *Il6*, and *Il1β*. Also induced were those genes encoding the NF-κB transcription factor subunits, *Nfkb1*, *Nfkb2*, and *Rela*. In addition, N-α-syn induced genes involved in other pathways, particularly those of the mitogen-activated pathway, as indicated by the induction of the immediate early genes, *Fos* and *Raf1*. At 4 h post-stimulation, expression of most NF-κB-related genes peaked. The majority of genes induced at 1 h remained elevated, with the addition of the apoptosis-regulatory genes *Card10* and *Casp8*. The NF-κB inhibitor, *Nfkbia*, was also induced (data not shown) but may become apparent only after removal or clearance of the stimulus, as *Ikbkb* expression was also induced at this time. Removal of N-α-syn from microglial cells after 4 h of stimulation reduced most NF-κB genes to prestimulatory levels. At 8 and 16 h following removal of N-α-syn from culture, several apoptosis-regulatory genes (*Card10*, *Card11*, and *Cflar*) were induced as well as genes for receptors of cell activation and NF-κB stimulation including *Tnfrsf1a* and *Cd40*. These results were similar but lesser in magnitude than stimulation of microglia

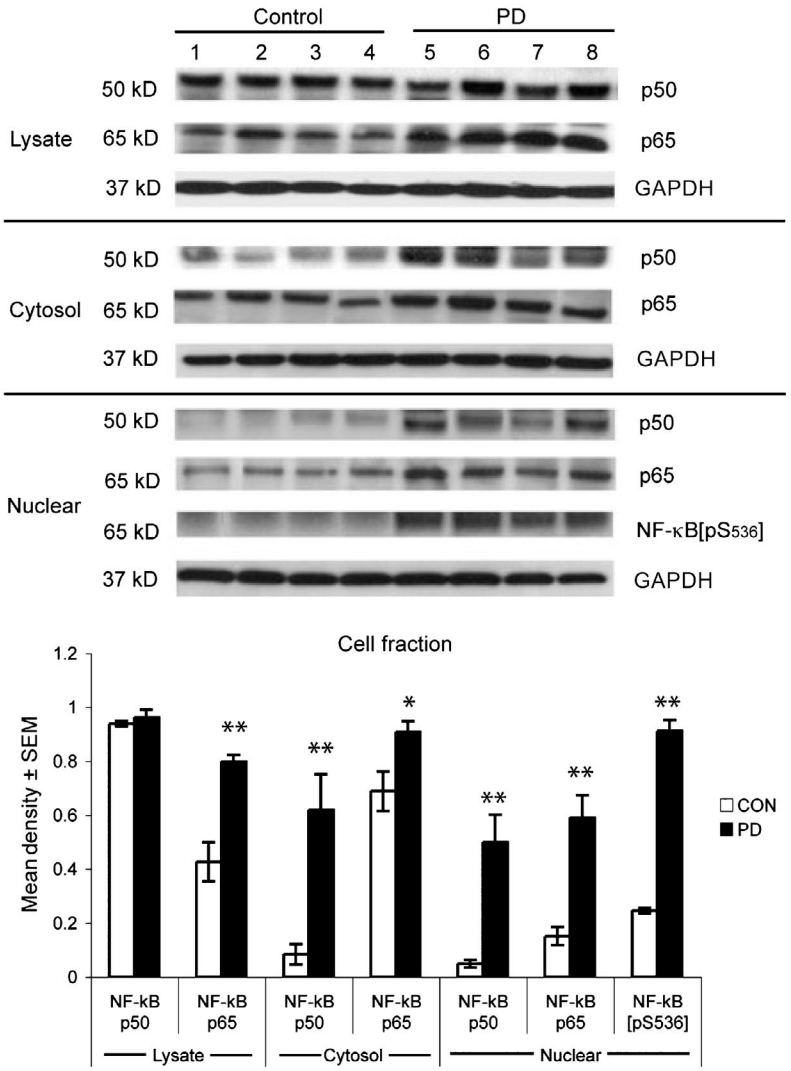

Figure 4. NF-κB translocation in PD. Expression of NF-κB subunits p50/NFKB1 and p65/RELA proteins were evaluated by western blot analysis from whole tissue lysates (top), cytosolic fractions (middle), and nuclear fractions (bottom) of SN from control and PD patients (Table 1). Expression of phosphorylated RELA/p65 [NF-κB pS536] within the nuclear fraction was also assessed. The mean densitometric values were determined with ImageJ software and normalized to GAPDH expression in the same sample (bottom). Values are represented as the mean density ± SEM for four patients/group and *p*-values of Student's *t*-test for pair-wise comparisons of densities from control (open bars) and PD (filled bars) patients are * $p < 0.05$ and ** $p < 0.005$. Blots are representative of two independent experiments ($n = 4$ patients per group).

with LPS (Figure 5b, Table 3). Consistent with microarray analyses, quantitative RT-PCR analyses of *Tnf*, *Il1β*, and *Ccl2* genes indicated very high levels of transcripts for these cytokines during stimulation by N-α-syn (10-, 3097-, and 16-fold increases, respectively) over pre-stimulatory levels (Figure 5c). Verification of gene expression during stimulation of other, less abundant, NF-κB-related genes were achieved, including *Tnfrsf1a* (6.2-fold increase), *Stat1* (2.3-fold increase), and *Rela* (3.6-fold increase). N-α-syn stimulation also increased expression of *Nos2* (inducible nitric oxide synthase) and Ifng (data not shown), both regulated by NF-κB activation. Expression of the neurotrophins *Bdnf* and *Gdnf* were also increased following N-α-syn stimulation.

N-α-syn-activated microglial proteome shows a reactive inflammatory phenotype

Analysis of the N-α-syn microglial transcriptome showed differential gene regulation and induction of the NF-κB pathway, indicative of an inflammatory microglial phenotype. Activation of this pathway influences downstream expression of proteins involved in processes including inflammation, immune regulation, survival, and proliferation. Protein expression obtained from cell lysates were analyzed following 2, 4, and 8 h of stimulation with 100 nmol/L N-α-syn to assess the translation of differences in gene induction to intracellular protein expression. Two-dimensional DIGE was used to compare protein expression profiles of unstimulated microglia (control) and N-α-syn-stimulated microglia (Figure 6). A complete listing of all proteins identified by LC-MS/MS is contained within Table 3.

Stimulation with N-α-syn resulted in differential expression of several proteins that are likely a consequence of NF-κB-related signaling pathways (Table 3) as soon as 2 h after stimulation. Many proteins differentially expressed could be attributed to oxidative stress, including the down-regulation of aconitase as well as the up-regulation of peroxiredoxin-1, -4, -5, superoxide dismutase, and heat-shock protein 70.

After 4 h of N-α-syn-stimulation, proteins decreased included several cytoskeletal proteins including β-actin,

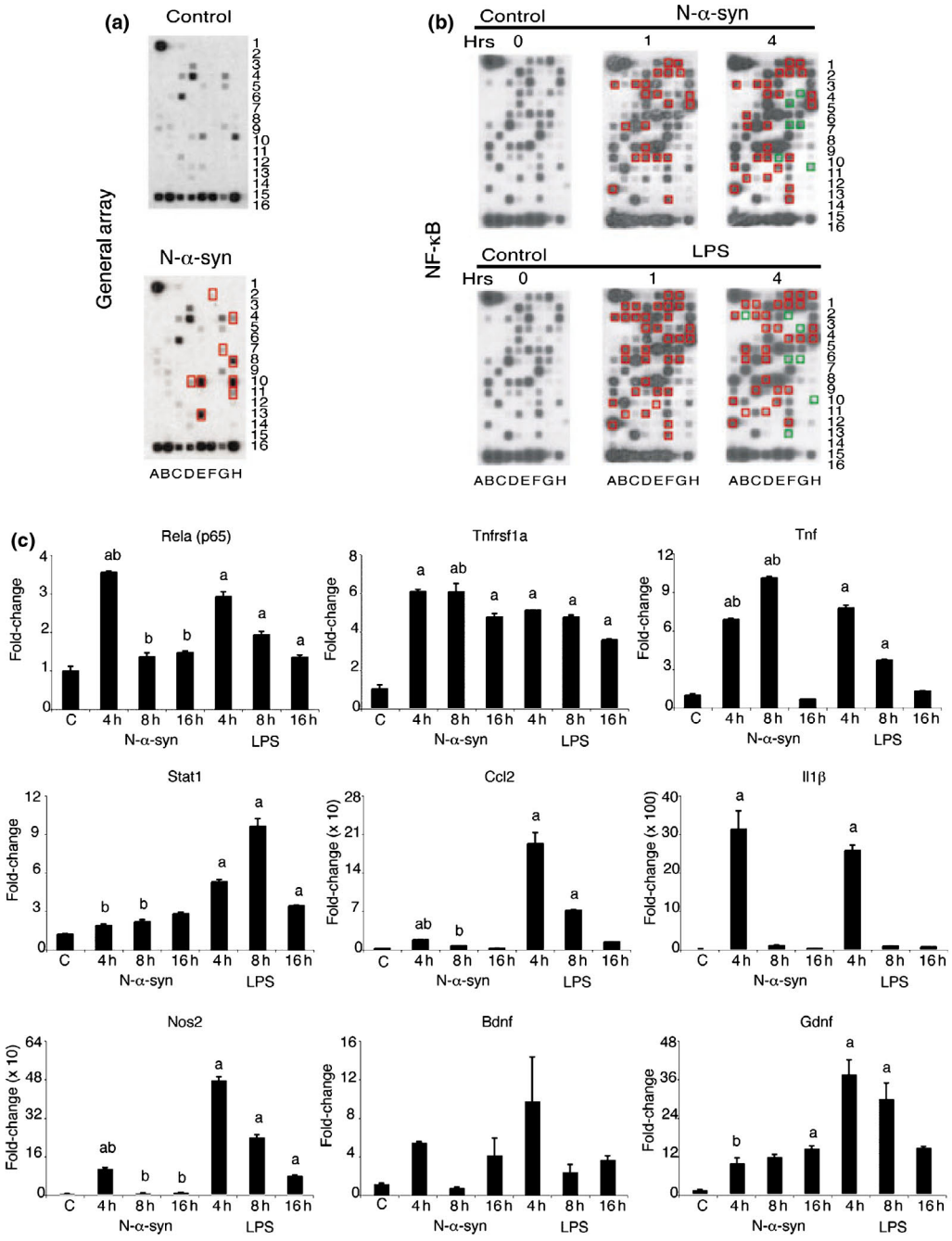

Figure 5. Microarray analysis of N-α-syn-stimulated microglia. RNA was isolated from microglial cells stimulated with 100 nmol/L N-α-syn or 100 ng/mL LPS from which cDNA was made and amplified. (**a**) General pathway-focused microarray revealed involvement of NF-κB signaling pathways. (**b**) Focused arrays were utilized for regulation of NF-κB associated genes for microglia that were unstimulated (0 h Control) or stimulated with 100 nmol/L N-α-syn or 100 ng/mL LPS for 1 h and 4 h, respectively. Red and green boxes indicate genes that were induced by stimulation at 1 and 4 h, respectively. Identified genes and their expression levels are shown in Table 1. (**c**) qPCR of mRNA from samples confirmed representative inductions for genes (rank and file position in microarry) *Ccl2* (F2), *Il1β* (H5), *Tnfrsf1a* (D13), *Stat1* (11E), *Rela* (10F), *Tnf* (A13), and *Nos2*. Gene expression for the neurotrophins *Bdnf* and *Gdnf* were also assessed by qPCR from the same mRNA/cDNA samples [$n = 3$, $p < 0.01$ compared with [a]0 h control (C) and [b]LPS at corresponding time point].

cofilin-1, profilin-1, tropomysin-3, and vimentin. The putative functions of other proteins decreased in N-α-syn-stimulated microglial lysates were found to be involved in cell adhesion and actin microfilament attachment to the plasma membrane (vinculin, coronin-1A, and adenylyl cyclase-associated protein 1), glycolysis and growth control (α-enolase), and migration (galectin 3 and macrophage migration inhibitory factor) (Walther *et al.* 2000;

Table 2. N-α-syn- and LPS-stimulated microglial transcriptome[a]

			N-α-syn (h)			LPS (h)		
Gene	Common name	NCBI[b]	4	8	16	4	8	16
Transcription factors								
Crebbp	Crebbp	12914	2.45			2.6		
Fos	c-Fos	14281	> 20					
Jun	c-Jun	16476	2.28					
Nfκb1	NFκB p50	18033	2.08			7.6		
Rel	Rel	19696	6.5			15.4	4.3	
Rela	NFκB p65	19697	4.59					
Smad3	Smad3	17127		−2.5				
Signal transduction								
Htr2b	Serotonin receptor	15559	3.56	−2.38				
Ikbkb	Ikbkb	16150	5.19			2.7		
Ikbke	Ikbke	56489	3.09					
Mapk3	Mapk3	26417	2.67					
Map3k14	Map3k14	53859		−2.34	−2.4	−2		
Plk2	Plk2	20620		2.39	2.04	3.1	4.1	2.5
Raf1	Raf-1	110157	5.63					
Stat1	Stat1	20846	5.56	3.5		5.1	5.2	3.2
Tbk1	Tbk1	56480	4.24					4.6
Tgfbr2	TGF-beta receptor 2	21813		−3.91		−2.8	−2.6	
Tlr2	Toll-like receptor 2	24088	7.38		2.43			
Tlr3	Toll-like receptor 3	142980		−2.2				
Tlr8	Toll-like receptor 8	170744	2.38					
Tnfrsf1a	TNFR1	21937		2.03	4.06	5.7	8.6	2.7
Inflammation								
Tnf	TNF-alpha	21926	2.25					
Ccl2	Chemokine ligand 2 (MCP-1)	20296	36.43	3.83	2.68	15.1	14.7	14.5
Il10	Interleukin 10	16153	2.31			5.8	4	3.1
Il1b	Interleukin 1-beta	16176	> 20	3.02	2.27	10.7	10.1	9.9
Il6	Interleukin 6	16193	13.09		2.57	78.1	25.4	2.3
Tnfrsf5	CD40	21939	9.91	25.6	7.23	145.1	135.5	45.7
Tnfrsf7	Tnfrsf7	21940		−3.14				
Traf6	Traf6	22034		−2.71				
Apoptosis								
Card10	Card10	105844	5.62	8.34	7.9	10.7	10.6	11.1
Card11	Card11	108723			2.63			
Card4	NOD1	107607	7.44			8.6	5.5	5.4
Casp1	Caspase 1	12362	4.3					
Casp8	Caspase 8	12370	2.49					
Cflar	Clarp	12633	19.65	2.22	2.08	8.6	7	6.7
Ripk1	Receptor (TNFRSF)-interacting serine-threonine kinase 1	19766		−2.6		2.1		
Malt1	Malt1	240354	6.1			6.2		
Ripk2	Cardiak	192656	6.16			9.5	7.3	
Tnfaip3	A20	21929			6.55	8.9	3.2	
Tnfsf10	TRAIL	22035		10.06				
Tradd	Tradd	71609			2.43	2.2		
Traf3	CD40BP	22031	2.03					
Other								
Csf2	GM-CSF	12981	3.76					
Dusp1	Dusp1	19252	3.15			6	6.2	5.3

Table 2. (continued)

Gene	Common name	NCBI[b]	N-α-syn (h) 4	8	16	LPS (h) 4	8	16
Hmgb1	Hmgb1	15289	2.96			2.2		
Icam1	Icam1	15894	12.79	4.97	3.46	5.2	4.8	3.8
C3	Complement component 3	12266	2.02					
Irak1	Interleukin-1 receptor-associated kinase 1	16179	2.19					
Lta	Lymphotoxin A	16992	3.09			22.8		

[a] Values represent fold-change versus unstimulated controls; [b] NCBI Entrez GeneID.

Chandrasekar *et al.* 2005). Annexin A3 is an inhibitor of phospholipase A2 and a promoter of apoptosis of inflammatory cells (Parente and Solito 2004), and was also down-regulated. The antioxidant glutaredoxin-1 was also decreased in cell lysates compared with unstimulated controls (Table 3). Four of the proteins increased in stimulated cell lysates affect intracellular calcium signaling, storage, and cell cycle regulation (swiprosin 1, calmodulin, calreticulum, and nucleophosmin 1) (Parente and Solito 2004; Vuadens *et al.* 2004; Meini *et al.* 2006).

By 8 h, 73 proteins were differentially expressed. Thirty-three proteins were decreased including all cytoskeletal proteins down-regulated at 4 h, vimentin and β-actin. Up-regulated proteins included the antioxidants superoxide dismutase, thioredoxin, and cytochrome c reductase. Oxidative stress can also lead to dysfunction of the proteasome and is implicated in PD pathogenesis (Gu *et al.* 2005). Indeed, as a result of N-α-syn stimulation the proteasome 26S subunit was decreased in these cell lysates, although ubiquitin and the ubiquitin conjugating enzyme E2N were increased, suggesting that the microglia may be compensating for decreased proteasomal activity (Table 3).

Neuroinflammatory Parkinson's disease phenotype

Analysis of the proteome of N-α-syn-stimulated microglia revealed the induction of NF-κB-related signaling pathways and initiation of several proteins involved in the cellular response to inflammation and oxidative stress. To investigate whether differential expression of proteins identified in our proteomic analyses of *in vitro* stimulated microglia was reflected in PD, protein expression of lysates prepared from the SN and BG (data not shown) of control and PD brains were assessed by western blot assays (Figure 7). Proteins increased in abundance within the secretome as a result of N-α-syn stimulation (A. D. Reynolds, I. Kadiu, S. G. Garg, J. G. Glanzer, T. Nordgen, R. Banerjee, P. Ciborowski, and H. E. Gendelman) were cross-validated in PD patients including calmodulin and the redox-associated secreted proteins biliverdin reductase and thioredoxin; whereas, secretion of the regulatory proteins glatectin-3 and 14-3-3σ, structural protein actin, and the redox protein glutathione-*S*-transferase were decreased following N-α-syn stimulation. These analyses verified the increased expression of calmodulin as well as the antioxidant biliverdin reductase in the SN of PD compared with age-matched controls without neurological disease. Actin expression appeared decreased in PD brains relative to controls, which coincided with our analysis of the N-α-syn-stimulated microglia secretome. In contrast to our *in vitro* results, expression of 14-3-3σ and galectin 3 were increased in PD brains. Glutathione-*S*-transferase expression was decreased in PD brains relative to control. Although expression of thioredoxin did not appear to be different within the SN, expression in the BG was significantly decreased in PD (data not shown). Proteins that were identified in the proteome of N-α-syn-stimulated microglia were, in part, also cross-validated in SN of PD and control brains. Akin to our laboratory model, expression of calmodulin was increased whereas expression of α-enolase (data not shown), L-plastin, α-tubulin, and actin were decreased in PD relative to control. The discrepancies between the cellular model and expression in the human tissue underscore the complexity of human disease and the multiple cell components that are involved. Indeed, comparing non-affected brains to PD brains may be misleading as already the proportion of cellular components are different, especially at end stage where greater than 80% of the dopaminergic neurons have died and substantial gliosis is present. However, overall these results support that the molecular and biochemical analyses of N-α-syn microglial activation appear, in part, applicable to human PD.

Discussion

Recent investigations (Biasini *et al.* 2004; Zhang *et al.* 2005; Zhou *et al.* 2005; Thomas *et al.* 2007) demonstrated that aggregated N-α-syn induces a neurotoxic inflammatory microglial phenotype that accelerates the demise of dopaminergic neurons, and as such, may contribute,

Table 3. N-α-syn-stimulated microglial proteome

Protein name	Mw (Da)[b]	PI[c]	Accession number[d]	Time (h)[e]	Number of peptides[f]	Volume ratio[g]
Proteins increased in N-α-syn-stimulated microglia cell lysates when compared with controls [a]						
Regulatory						
10 kDa Heat-shock protein, mitochondrial	10 825	8.18	Q64433	8	6	3.45
S100 calcium-binding protein A13	11 151	5.89	P97352	8	2	5.57
Apoptosis-associated speck-like protein containing a CARD	21 459	5.26	O88597	2	6	1.58
Beclin-1	51 534	4.89	O88597	2	2	1.48
Calmodulin	16 706	4.09	P62156	8	3	7.51
Calreticulin	47 995	4.33	P14211	8	7	1.67
Cystatin B	11 039	6.82	Q62426	8	2	3.06
Dynein light chain 2A	10 852	6.86	P62627	8	3	3.73
Ef3-CaM	16 578	4.04	P99027	2	8	2.26
Eukaryotic initiation factor 5A isoform I variant D	16 821	5.08	Q7L7L3	4	2	1.51
Fatty acid-binding protein	14 996	6.18	Q05816	2	3	3.17
Heat-shock 70 kDa protein 1A	70 052	5.48	Q9EPB4	4	2	1.43
Heat-shock 70 kDa protein 1B	70 167	5.53	P17879	4	2	1.79
Heat-shock 70 kDa protein 1L	70 637	5.91	P16627	8	2	1.79
Histone H2B F	13 805	10.32	P10853	2	2	4.07
Kinesin light chain 4	68 613	5.76	Q5JQI4	8	2	1.85
Mitogen-activated protein-binding protein-interacting protein	13 472	5.3	Q9JHS3	8	2	4.75
Nucleophosmin 1	32 558	4.62	Q5U438	8	9	1.68
SH3 domain-binding glutamic acid-rich-like protein 3	10 470	5.02	Q91VW3	8	4	3.12
SWIPROSIN 1/EF hand domain containing protein 2 (Efhd2)	26 800	5.07	Q8C845	8	2	2.06
Ubiquitin	8560	6.56	P62990	8	2	4.88
Structural/cytoskeletal						
Capg protein	39 240	6.73	P24452	8	11	1.71
Capping protein	38 691	6.73	Q3TNN6	4	2	1.24
Cofilin-1	18 401	8.26	P45592	2	5	3.28
Destrin	18 378	8.2	Q9R0P3	8	6	3.04
Myosin heavy	223 083	5.64	P02564	4	2	1.27
Talin	110 842	5.94	Q3TBC3	2, 4	4	1.58
Tubulin alpha-1 chain	50 152	4.94	P68361	8	7	1.92
Redox						
Isovaleryl-CoA dehydrogenase	46 325	8.53	Q9JHI5	8	7	1.71
Cytochrome c oxidase, subunit Vb	13 838	8.34	Q9D881	8	3	3.98
Peroxiredoxin-1	22 176	8.26	P35700	2	20	1.42
Peroxiredoxin-4	31 053	6.67	O08807	2	2	1.42
Peroxiredoxin-5	21 897	9.1	P99029	2	2	1.48
Superoxide dismutase	24 603	8.8	P09671	2	2	1.42
Enzymes						
Cathepsin C	52 347	6.41	Q3TIF1	4	2	1.29
Cathepsin Z	34 175	6.13	Q9ES94	8	4	1.69
Ferritin heavy chain	20 935	5.53	P09528	2	4	1.44
Hexosaminidase B	61 115	8.28	P20060	2	8	2.67
Peptidyl-prolyl cis-trans isomerase A	17 960	7.74	P17742	8	14	4.77
Ubiquitin-conjugating enzyme E2N	17 127	6.13	P61089	8	5	3.26
Ubiquitin-conjugating E2 Q2	42 192	4.9	Q7YQJ9	4	5	1.3
Vacuolar ATP synthase subunit G1	13 362	5.52	Q9D1K2	8	3	4.23

Table 3. (continued)

Protein name	Mw (Da)[b]	PI[c]	Accession number[d]	Time (h)[e]	Number of peptides[f]	Volume ratio[g]
Other						
Annexin A5	35 752	4.83	P48036	8	4	1.7
39S ribosomal protein L12	21 695	9.34	Q9DB15	4	3	1.26
Apolipoprotein A	35 853	5.56	Q6GTX3	8	5	1.73
Fatty acid-binding protein (E-FABP)	15 006	6.18	Q05816	8	2	3.52
Fibulin 2	126 414	4.55	Q3TGL4	8	2	5.57
Heterogenous nuclear ribonucleoprotein K	50 976	5.39	P61979	8	8	1.69
Prosaposin	61 086	5.11	Q3TID4	8	3	10.1
Proteins decreased in N-α-syn-stimulated microglial cell lysates [a]						
Regulatory						
14-3-3 Protein epsilon	29 155	4.63	P62259	8	8	−3.33
26S protease regulatory subunit 7	48 517	5.72	P46472	8	2	−2.4
Acyl-CoA binding protein	9863	8.78	P31786	4	8	−3
Adenylyl cyclase-associated protein 1	51 444	7.3	P40124	8	9	−1.9
Centromere protein F	367 594	5.03	P49454	2	3	−1.68
Chloride intracellular channel protein 1	26 865	5.09	Q9Z1Q5	8	3	−3.28
Coronin1B	53 912	5.54	Q9WUM3	4	3	−1.26
Eukaryotic translation initiation factor 3	35 586	5.69	Q3THA0	8	2	−3.32
Galectin 3	27 384	8.5	P16110	4	13	−2.34
Heterogenous nuclear ribonucleoproteins A2/B1	35 992	8.67	O88569	2	5	−1.61
Macrophage Migration Inhibitory factor	12 373	7.28	P34883	8	3	−2.03
Nuclear migration protein nudC	38 334	5.17	O35685	8	7	−4.13
Programmed cell death 6-interacting protein	96 010	6.15	Q9WU78	4	8	−1.25
SH3 domine-binding Glutamic acid-rich-like protein	10 477	5.02	Q91VW3	8	12	−1.81
Synaptotagmin-like protein 2	106 806	6.14	Q99N50	2	2	−1.46
Structural/cytoskeletal						
Beta-actin	41 737	5.78	P60710	4	26	−3.69
Coronin-1A	50 989	6.05	O89053	8	10	−2.4
Desmin	53 334	5.21	P31001	8	13	−3.25
Gamma actin-like protein	43 572	5.11	Q9QZ83	8	27	−4.03
Gelsolin	80 712	5.47	Q3U9Q8	8	7	−3.3
L Plastin	70 018	5.2	Q61233	8	15	−2.58
MFLJ00343 protein	205 326	5.6	Q6KAM8	8	17	−2.12
Profilin-1	14 816	8.5	P62962	8	7	−1.35
Tropomodulin	40 441	5.02	Q3KP84	8	2	−4.13
Tropomysin-3	33 149	4.73	P21107	4	10	−1.25
Tubulin alpha 4	49 761	4.95	Q3TY31	8	7	−3.23
Tubulin alpha 6	49 907	4.96	QTIZ0	8	9	−3.25
Vimentin	53 689	5.03	Q3TFD9	8	88	−3.38
Redox						
Glutaredoxin 1	11 732	8.69	Q91V76	4	2	−1.7
Thioredoxin domain containing 5	46 386	5.51	Q3TEE8	8	38	−4.24
Enzyme						
α-Enolase	47 010	6.36	P17182	8	8	−2.4
2′-5′ olygoadenylate synthetase 1F	42 270	7.09	Q8K465	2	7	−1.68
3-ketoacyl-CoA thiolase A	43 935	8.74	Q921H8	8	3	−2.66
Aconitase	98 152	5.98	Q42560	2	3	−1.59
ATP synthase	59 751	9.16	Q53XX6	2	2	−1.55
ATP synthase e chain	8099	9.34	Q06185	4	5	−1.52
Carbonyl reductase	30 394	6.15	Q8K354	4	3	−1.27
Cathepsin B	37 256	5.57	P10605	8	15	−3.34
Cathepsin D	44 925	6.71	P18242	8	34	−3.68
Cathepsin S	38 707	6.51	Q8BSZ5	4	3	−1.29

Table 3. (continued)

Protein name	Mw (Da)[b]	PI[c]	Accession number[d]	Time (h)[e]	Number of peptides[f]	Volume ratio[g]
F1-ATPase alpha subunit	44 144	7.07	O78824	2	9	−1.55
Fructose-bisphosphate aldolase A	39 225	8.4	P05064	8	33	−2.66
Glutamate oxaloacetate transaminase 2	47 183	9.05	Q3TIP6	4	3	−1.23
Phosphomannomutase 2	27 625	6.01	Q9D1M5	4	3	−1.3
Succinyl-CoA ligase beta chain, mitochondrial	50 082	6.57	Q9Z219	8	3	−4.12
Transitional endoplasmic reticulum ATPase	53 524	4.14	Q01853	8	19	−3.31
Other						
Annexin A1	38 603	7.15	P10107	8	8	−1.9
Annexin A3	36 240	5.33	O35639	8	5	−1.93
28S ribosomal protein S12, mitochondrial	15 437	10.72	O35680	2	2	−1.63
Arcn1 protein	47 964	5.61	Q8R1S6	8	7	−1.93
Beta-galactoside-binding lectin	15 914	9.01	Q61357	4	7	−1.84
Centrosomal protein of 27 kDa	26 839	6.06	Q9CQS9	2	3	−1.68
Clathrin light chain B	25 171	4.56	Q6IRU5	2	3	−1.68
Density regulated protein	22 152	5.21	Q9CQJ6	8	2	−3.48
Fatty acid binding protein	14 996	6.18	Q05816	4	4	−1.27
Glycoprotein (transmembrane) nmb	63 577	7.88	Q3TAV1	8	2	−3.13
Gsn protein	80 763	5.52	Q6PAC1	8	13	−1.66
Histone H2A type 1	14 004	11.05	P22752	8	2	−5.46
Protective protein for beta-galactosidase	53 795	5.56	Q9D2D1	4	3	−3.47
Vinculin	116 586	5.77	Q64727	8	9	−1.82

[a] The CID spectra were compared against those of the EMBL non-redundant protein database by using SEQUEST (ThermoElectron, San Jose, CA, USA). After filtering the results based on cross-correlation Xcorr (cutoffs of 2.0 for [M + H]1+, 2.5 for [M + 2H]2+, and 3.0 for [M + 3H]3+), peptides with scores greater than 3000 and meeting delta cross-correlation scores (ΔCn) > 0.3, and fragment ion numbers > 60% were deemed valid by these SEQUEST criteria thresholds, which have been determined to afford greater than 95% confidence level in peptide identification; [b] Theoretical molecular mass; [c] Isoelectric point; [d] Accession numbers for UniProt (accessible at http://www.ipr.uniprot.org/search/textSearch.shtml);[e] Hours following stimulation with N-α-syn; [f] Number of peptides identified for each protein selected based on the above mentioned criteria; [g] Volume ratio indicates fold-change versus control.

in part, to PD progression. However, the mechanisms underlying N-α-syn-mediated microglial neurotoxicity remain obscure. To investigate the means by which N-α-syn-mediated microglial activation affects dopaminergic neurodegeneration, the molecular and biochemical signatures of N-α-syn-stimulated microglia were investigated. This report now demonstrates that microglial stimulation with aggregated, nitrated α-syn leads to a neuroinflammatory phenotype capable of mediating neuronal toxicity. These observations are consistent with the notion that release of this protein from injured neurons can lead to microglial activation and nigrostriatal degeneration, reflective of PD pathobiology. A key component of this study was the integration of physiologic, genomic, and proteomic techniques to develop a fingerprint of microglial cell activation following its interactions with N-α-syn. This microglia phenotype was characterized by morphological changes, as well as alterations in both the transcriptome and proteome that result in reactive microgliosis and secretion of bioactive factors, which were neurotoxic. Moreover, our examination shows human correlates of disease while permitting an integrated cross-disciplinary approach for describing a microglial "fingerprint" that may be reminiscent of inflammatory processes in PD. The inflammatory microglial phenotype now shown follows its interaction with N-α-syn and may affect dopaminergic neurodegeneration.

Microglia normally function as debris scavengers, killers of microbial pathogens, regulators of the immune responses, and supporters of neuronal functions (Vilhardt 2005); all necessary for host defense. However, during neurodegenerative diseases, their phenotype is altered by uncontrolled activation. Substantial evidence for reactive microglia in and around dead or dying dopaminergic neurons in the SN of PD patients suggests that microglial activation and concomitant secretion of neurotoxic factors play a role in the nigrostriatal degeneration that occurs in PD. Stimulation by environmental cues that include aggregated proteins and inflammatory factors often results in the robust secretion of toxic factors that accelerate neuronal injury and death (McGeer and McGeer 1998; Liu and Hong 2003). Cytokines released from activated microglia bind their cognate receptor on dopaminergic neurons to activate signal trans-

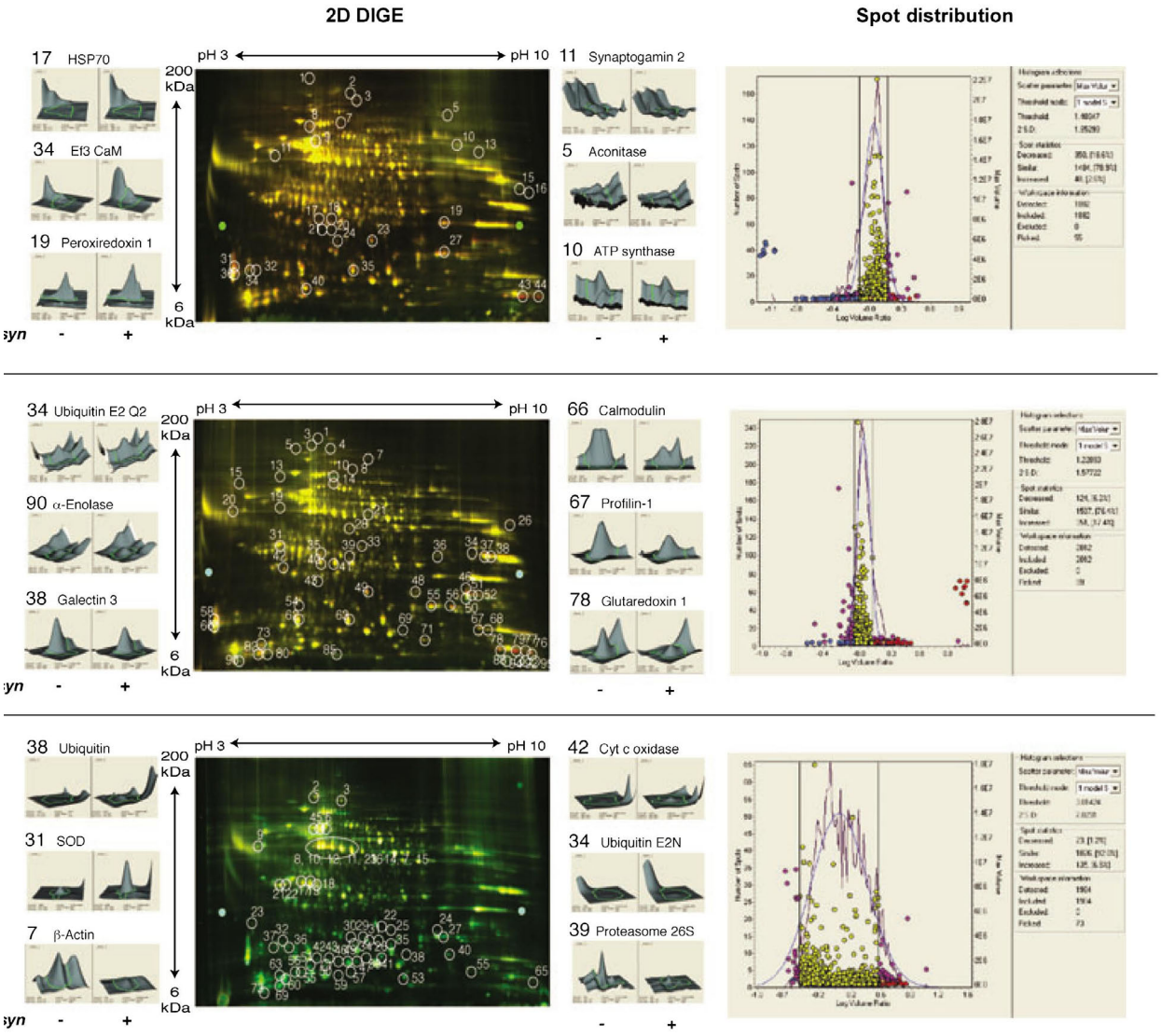

Figure 6. 2DE and LC-MS/MS analysis of the N-α-syn-stimulated microglia proteome. Fluorescence 2D DIGE analysis of N-α-syn-activated microglial cell lysates. Fluorescence 2D DIGE (2DE) analysis of activated microglial cell lysates at 2, 4, and 8 h after N-α-syn stimulation. Proteins from cell lysates of unstimulated microglia labeled with Cy3 appear green on the 2 dimensional gels, while proteins of N-α-syn stimulated microglia labeled with Cy5 appear red, and proteins common to both appear yellow. Three-dimensional DeCyder interpretation for six representative proteins per time-point are shown. The numbers correspond to the protein spot labeled on gels. Analysis of spot distribution to locate and define protein spots (right panel). Protein spots from samples of stimulated cell lysates were identified as decreased (blue), increased (red), or common (yellow) versus non-stimulated cell lysates. Spots picked for sequencing analysis with LC-MS/MS are shown in purple. Abbreviations: HSP70, heat-shock protein 70; Cyt c oxidase, cytochrome c oxidase; SOD, superoxide dismutase. A complete listing of all proteins identified through 2DE is contained within Table 3.

duction pathways resulting in apoptosis or necrosis. The persistent activation of microglia in response to dopaminergic neuron injury has been investigated extensively using the neurotoxin, MPTP. Work from several laboratories has documented that microglia activation accounts for ~90% of MPTP-induced neuronal death (Wu *et al.* 2003; McGeer and McGeer 2004). Furthermore, studies show MPTP neurotoxicity may be attenuated in mice unable to mount pro-inflammatory responses (Feng *et al.* 2002; Sriram *et al.* 2002; Teismann *et al.* 2003; Wu *et al.* 2003), by treatment with anti-inflammatory drugs (Liu *et al.* 2006) and antioxidants (Zbarsky *et al.* 2005), blockage of the NF-κB pathway (Ghosh *et al.* 2007), or by induction of a regulatory T-cell response (Benner *et al.* 2004; Laurie *et al.* 2007; Reynolds *et al.* 2007); all converging on attenuating microglial activation. In contrast, exacerbation of microglial activation by infiltrating effector lymphocytes to modified self-peptides may worsen MPTP-induced neurodegeneration (E. J. Benner, R. Banerjee, A. D. Reynolds, S. Sherman, V. M. Pisarev, V. Tsiperson, C.

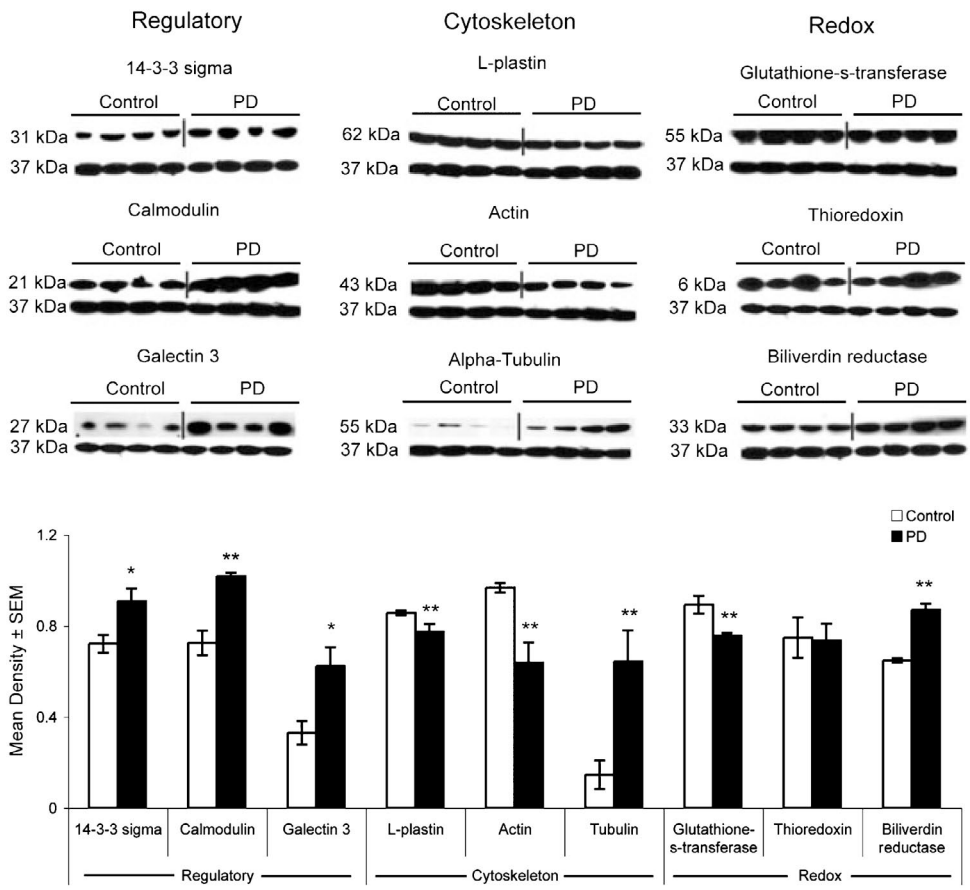

Figure 7. N-α-syn-stimulated microglial proteins in PD brain tissue. Immunoblot identification of proteins in the SN and BG of PD brains that were previously observed in N-α-syn-stimulated microglia. This includes 14-3-3σ, calmodulin, galectin-3, L-plastin, actin, tubulin, glutathione-*S*-transferase, thioredoxin, and biliverdin reductase. The proteins are divided into regulatory, cytoskeleton, or redox functions. The mean densitometric values were determined with ImageJ software and normalized to GAPDH expression in the same sample (bottom). Values are represented as the mean density ± SEM for four patients/group and *p*-values of Student's *t*-test of pair-wise comparisons of densities from Control (open bars) and PD (closed bars) patients are * $p < 0.05$ (** $p < 0.05$ and congruent results with the N-α-syn-microglial proteomic and western blot assays).

Nemacheck, P. Ciborowski, S. Przedborski, R. L. Mosley, and H. E. Gendelman, unpublished data).

Generation of reactive molecular species by microglia, as well as changes that occur during dopamine metabolism and mitochondrial function can result in oxidation and nitration of proteins, DNA modifications, and lipid peroxidation. Oxidation and nitration of α-syn leads to formation of aggregates and the stabilization of assembled filaments found to be a major component of LBs, the hallmark lesions of PD. The results of the present study, as well as research performed by others (Biasini *et al.* 2004; Zhang *et al.* 2005; Zhou *et al.* 2005; Thomas *et al.* 2007) support the hypothesis that microglia activated by N-α-syn is a component of an inflammatory cascade that perpetuates nigrostriatal degeneration in PD. *First*, nitrated α-syn was identified in extracts from the SN of PD patients in copious concentrations relative to control and AD brains. *Second*, α-syn aggregates released from LB during dopaminergic neuronal death can interact with adjacent microglial cells found in abundance within the SNpc of PD patients (Spillantini *et al.* 1997; McGeer and McGeer 1998; Croisier *et al.* 2005). Alternatively, α-syn may also be released or secreted from the cytosol of dopaminergic cells into the extracellular environment where it is more prone to aggregation and oxidative damage (Kakimura *et al.* 2001; Lee *et al.* 2005; Sung *et al.* 2005). *Third*, microglial activation is associated with degenerating dopaminergic neurons and deposition of α-syn in the SN of PD patients (Croisier *et al.* 2005). *Fourth*, native and nitrated α-syn activate microglia with release of ROS and induce neurotoxicity as shown herein and by others (Zhang *et al.* 2005; Thomas *et al.* 2007). *Fifth*, recent evidence supports that N-α-syn drains to the cervical lymph nodes, availing it for processing and presentation by antigen-presenting cells to the adaptive immune system, which in turn can circumvent or break immu-

nological tolerance to direct immune responses that possibly contribute to prolonged microglial activation and neurodegeneration (E. J. Benner, R. Banerjee, A. D. Reynolds, S. Sherman, V. M. Pisarev, V. Tsiperson, C. Nemacheck, P. Ciborowski, S. Przedborski, R. L. Mosley, and H. E. Gendelman, unpublished data). Moreover, α-syn and its modified forms are present in extracellular biological fluids including human plasma (El-Agnaf *et al.* 2003) and are proposed as biomarkers for disease (Fjorback *et al.* 2007). Evidence of systemic complications associated with PD including abnormal gastrointestinal function (Bassotti *et al.* 2000), cardiac denervation, and orthostatic hypotension (Taki *et al.* 2000; Goldstein *et al.* 2005) further suggest a peripheral component in disease. Taken together, this work extends those of others (Wang *et al.* 2005; Zhou *et al.* 2005; McLaughlin *et al.* 2006). By using proteomic analyses for examination of the activated microglial proteome it provides human disease correlates while permitting an integrated cross-disciplinary proteomic approach towards elucidating a PD microglial "fingerprint." The work provides evidence that such a profile is inflammatory and may be linked to neurotoxicity. However, one must exert caution in over interpreting these experimental results. Nonetheless, whether or not these findings are directly linked to the pathogenesis of PD will certainly require further study. Although clear evidence is provided that microglial activation is part of PD whether this process is a secondary by-product of ongoing neurodegeneration or a primary inducer of disease remains uncertain.

Parallels are demonstrated herein between N-α-syn and LPS for microglial activation and support a commonality for innate immune responses in disease. The findings suggest that pro-inflammatory processes may be common amongst mononuclear phagocytes that see disparate activators. LPS is a strong activator of microglia both *in vivo* and *in vitro*. A single systemic exposure to LPS can lead to neuroinflammation associated with increased expression of pro-inflammatory cytokines, NADPH oxidase-mediated release of superoxide (Gao *et al.* 2002), and activation of the NF-κB pathway (Qin *et al.* 2007) resulting in neurodegeneration. Microglial activation by LPS and N-α-syn were associated with induction of the NF-κB and mitogen activation pathways, characteristic of an inflammatory phenotype. However, key differences in the inflammatory responses induced by LPS or N-α-syn were identified, including genes involved in signal transduction and apoptosis, as well as induction of an inflammatory response that was greater in magnitude after stimulation with LPS compared with that of N-α-syn. It is possible that the differences in transcription may be dose or pathway dependent as the stimulatory capacity and pathways activated by the two stimuli may differ significantly. Having demonstrated that N-α-syn stimulation induces microglial activation, this model may be used to study PD and reflect the unique molecular changes that occur during disease progression.

Our finding suggests that modifications to α-syn may be a common denominator for microglial activation in sporadic and familial PD. These observations also identify prospective pathways that are associated with PD and as such uncover potential targets for therapeutic intervention. For instance, identification of NF-κB activation by microglia in response to divergent stimuli suggests that activation of NF-κB and its related signaling pathways may be a key component in the inflammatory response leading to neuronal death. The microglial response to N-α-syn was linked to neurotoxicity. Nonetheless, we also showed proteomic fingerprints that were potentially protective. These include antioxidants and growth factors. Although considered to be a necessary component of CNS homeostasis, the potentially protective microglia mechanisms are lost as PD progresses uncontrolled. Furthermore, the similarities and differences found between the acute *in vitro* model of N-α-syn microglial stimulation and what is present in PD brains support that ongoing inflammatory responses present in disease may affect CNS protective responses. The observations of sustained NF-κB activation and differential expression of regulatory, structural, and redox proteins at end-stage disease support, in part, a persistent inflammatory process that could affect dopaminergic loss.

In summary, a mechanistic role for aggregated N-α-syn in stimulating a neurotoxic microglial phenotype was observed. In this 'potential' scheme, a pathogenic paracrine loop of immune activation occurs consisting of dopaminergic neuronal injury or death, release of aggregated N-α-syn from the cytosol or LB either through exocytosis or neuronal degeneration into the extracellular milieu, microglial activation with release of toxic factors which, may ultimately lead to further neuronal injury and sustained α-syn release. Regardless of concurrent pathogenic events in PD, which initiate dopaminergic degeneration or the mechanisms associated with activation by N-α-syn, the resultant activation of resident microglia could, in part, perpetuate neuronal injury and subsequent disease progression. Thus, the perpetual presence of activated microglia, left uncontrolled, may consistently confound PD therapies. Our investigations also provide a novel approach towards elucidating cellular immune responses for neurodegeneration and suggest potential molecular targets to slow disease processes.

Acknowledgments

We thank Dr E. Benner for providing recombinant mouse α-synuclein, Dr S. Appel for providing the MES23.5 cell line, and L. Shlyahtenko for preparing the AFM images and the cell analysis facility for flow cytometric analyses. We are deeply indepted to Drs Susan Morgello and Eliezer Masliah and the National Research Tissue Consortium for help in providing the human brain autopsy tissues. The work was supported by the Frances and Louis Blumkin Foundation, the Commu-

nity Neuroscience Pride of Nebraska Research Initiative, and the Alan Baer Charitable Trust (to HEG), a University of Nebraska Medical Center Graduate Student Excellence Award (to ADR), Michael J. Fox Foundation (to RLM), and NIH grants 1T32 NS07488 (to ADR and HEG), 1R21 NS049264 (to RLM), 2R37 NS36136, PO1 NS43985, PO1 MH64570, R01 MH79886 (to HEG), and R24 NS45491 and R01 MH79886 (to BG).

References

Backman C. M., Shan L., Zhang Y. J., Hoffer B. J., Leonard S., Troncoso J. C., Vonsatel P. and Tomac A. C. (2006) Gene expression patterns for GDNF and its receptors in the human putamen affected by Parkinson's disease: a real-time PCR study. Mol. Cell. Endocrinol. 252, 160–166.

Bal-Price A. and Brown G. C. (2001) Inflammatory neurodegeneration mediated by nitric oxide from activated glia-inhibiting neuronal respiration, causing glutamate release and excitotoxicity. J. Neurosci. 21, 6480–6491.

Banati R. B. D. S. and Blunt S. B. (1998) Glial pathology but absence of apoptotic nigral neurons in long-standing Parkinson's disease. Mov. Disord. 13, 221–227.

Bassotti G., Maggio D., Battaglia E., Giulietti O., Spinozzi F., Reboldi G., Serra A. M., Emanuelli G. and Chiarioni G. (2000) Manometric investigation of anorectal function in early and late stage Parkinson's disease. J. Neurol. Neurosurg. Psychiatry 68, 768–770.

Benner E. J., Mosley R. L., Destache C. J., Lewis T. B., Jackson-Lewis V., Gorantla S., Nemachek C., Green S. R., Przedborski S. and Gendelman H. E. (2004) Therapeutic immunization protects dopaminergic neurons in a mouse model of Parkinson's disease. Proc. Natl Acad. Sci. USA 101, 9435–9440.

Biasini E., Fioriti L., Ceglia I., Invernizzi R., Bertoli A., Chiesa R. and Forloni G. (2004) Proteasome inhibition and aggregation in Parkinson's disease: a comparative study in untransfected and transfected cells. J. Neurochem. 88, 545–553.

Block M. L. and Hong J. S. (2005) Microglia and inflammation-mediated neurodegeneration: multiple triggers with a common mechanism. Prog. Neurobiol. 76, 77–98.

Chandrasekar I., Stradal T. E., Holt M. R., Entschladen F., Jockusch B. M. and Ziegler W. H. (2005) Vinculin acts as a sensor in lipid regulation of adhesion-site turnover. J. Cell Sci. 118, 1461–1472.

Chartier-Harlin M. C., Kachergus J., Roumier C. *et al.* (2004) Alpha-synuclein locus duplication as a cause of familial Parkinson's disease. Lancet 364, 1167–1169.

Choi D. K., Pennathur S., Perier C. *et al.* (2005) Ablation of the inflammatory enzyme myeloperoxidase mitigates features of Parkinson's disease in mice. J. Neurosci. 25, 6594–6600.

Cicchetti F., Brownell A. L., Williams K., Chen Y. I., Livni E. and Isacson O. (2002) Neuroinflammation of the nigrostriatal pathway during progressive 6-OHDA dopamine degeneration in rats monitored by immunohistochemistry and PET imaging. Eur. J. Neurosci. 15, 991–998.

Croisier E., Moran L. B., Dexter D. T., Pearce R. K. and Graeber M. B. (2005) Microglial inflammation in the parkinsonian substantia nigra: relationship to alpha-synuclein deposition. J. Neuroinflammation 2, 14.

Dauer W. and Przedborski S. (2003) Parkinson's disease: mechanisms and models. Neuron 39, 889–909.

Dobrenis K. (1998) Microglia in cell culture and in transplantation therapy for central nervous system disease. Methods 16, 320–344.

Du Y., Ma Z., Lin S. *et al.* (2001) Minocycline prevents nigrostriatal dopaminergic neurodegeneration in the MPTP model of Parkinson's disease. Proc. Natl Acad. Sci. USA 98, 14669–14674.

El-Agnaf O. M., Salem S. A., Paleologou K. E. *et al.* (2003) Alpha-synuclein implicated in Parkinson's disease is present in extracellular biological fluids, including human plasma. FASEB J. 17, 1945–1947.

Fahn S. and Sulzer D. (2004) Neurodegeneration and neuroprotection in Parkinson disease. NeuroRx 1, 139–154.

Fahn S., Clarence-Smith K. E. and Chase T. N. (1998) Parkinson's disease: neurodegenerative mechanisms and neuroprotective interventions – report of a workshop. Mov. Disord. 13, 759–767.

Feng Z. H., Wang T. G., Li D. D., Fung P., Wilson B. C., Liu B., Ali S. F., Langenbach R. and Hong J. S. (2002) Cyclooxygenase-2-deficient mice are resistant to 1-methyl-4-phenyl1, 2, 3, 6-tetrahydropyridine-induced damage of dopaminergic neurons in the substantia nigra. Neurosci. Lett. 329, 354–358.

Fjorback A. W., Varming K. and Jensen P. H. (2007) Determination of alpha-synuclein concentration in human plasma using ELISA. Scand. J. Clin. Lab. Invest. 67, 431–435.

Forno L. S. D. L., Irwin I., Di Monte D. and Langston J. W. (1992) Astrocytes and Parkinson's disease. Prog. Brain Res. 94, 429–436.

Gao H. M., Hong J. S., Zhang W. and Liu B. (2002) Distinct role for microglia in rotenone-induced degeneration of dopaminergic neurons. J. Neurosci. 22, 782–790.

Ghosh A., Roy A., Liu X., Korodower J. H., Mufson E. J., Mosley R. L., Gendelman H. E., Ghosh S. and Pahan K. (2007) Selective inhibition of NF-kB activation prevents dopaminergic neuronal loss in a mouse model of Parkinson's disease. Proc. Natl Acad. Sci. In press.

Giasson B. I., Duda J. E., Murray I. V., Chen Q., Souza J. M., Hurtig H. I., Ischiropoulos H., Trojanowski J. Q. and Lee V. M. (2000) Oxidative damage linked to neurodegeneration by selective alpha-synuclein nitration in synucleinopathy lesions. Science 290, 985–989.

Giulian D., Li J., Bartel S., Broker J., Li X. and Kirkpatrick J. B. (1995) Cell surface morphology identifies microglia as a distinct class of mononuclear phagocyte. J. Neurosci. 15, 7712–7726.

Goedert M. (1999) Filamentous nerve cell inclusions in neurodegenerative diseases: tauopathies and alpha-synucleinopathies. Philos. Trans. R. Soc. Lond. B Biol. Sci. 354, 1101–1118.

Goldstein D. S., Eldadah B. A., Holmes C., Pechnik S., Moak J., Saleem A. and Sharabi Y. (2005) Neurocirculatory abnormalities in Parkinson disease with orthostatic hypotension: independence from levodopa treatment. Hypertension 46, 1333–1339.

Gu Z., Nakamura T., Yao D., Shi Z. Q. and Lipton S. A. (2005) Nitrosative and oxidative stress links dysfunctional ubiquitination to Parkinson's disease. Cell Death Differ. 12, 1202–1204.

Halliday G. M., Ophof A., Broe M., Jensen P. H., Kettle E., Fedorow H., Cartwright M. I., Griffiths F. M., Shepherd C. E. and Double K. L. (2005) Alpha-synuclein redistributes to

neuromelanin lipid in the substantia nigra early in Parkinson's disease. Brain 128, 2654–2664.

Hong J. S. (2005) Role of inflammation in the pathogenesis of Parkinson's disease: models, mechanisms, and therapeutic interventions. Ann. NY Acad. Sci. 1053, 151–152.

Hornykiewicz O. and Kish S. J. (1987) Biochemical pathophysiology of Parkinson's disease. Adv. Neurol. 45, 19–34.

Kakimura J., Kitamura Y., Takata K., Kohno Y., Nomura Y. and Taniguchi T. (2001) Release and aggregation of cytochrome c and alpha-synuclein are inhibited by the antiparkinsonian drugs, talipexole and pramipexole. Eur. J. Pharmacol. 417, 59–67.

Kruger R., Kuhn W., Muller T., Woitalla D., Graeber M., Kosel S., Przuntek H., Epplen J. T., Schols L. and Riess O. (1998) Ala30Pro mutation in the gene encoding alpha-synuclein in Parkinson's disease. Nat. Genet. 18, 106–108.

Kurkowska-Jastrzebska I., Litwin T., Joniec I., Ciesielska A., Przybylkowski A., Czlonkowski A. and Czlonkowska A. (2004) Dexamethasone protects against dopaminergic neurons damage in a mouse model of Parkinson's disease. Int. Immunopharmacol. 4, 1307–1318.

Laurie C., Reynolds A., Coskun O., Bowman E., Gendelman H. E. and Mosley R. L. (2007) CD4+ T cells from Copolymer-1 immunized mice protect dopaminergic neurons in the 1-methyl-4-phenyl-1,2,3,6-tetrahydropyridine model of Parkinson's disease. J. Neuroimmunol. 183, 60–68.

Lee H. J., Patel S. and Lee S. J. (2005) Intravesicular localization and exocytosis of alpha-synuclein and its aggregates. J. Neurosci. 25, 6016–6024.

Liu B. and Hong J. S. (2003) Role of microglia in inflammation-mediated neurodegenerative diseases: mechanisms and strategies for therapeutic intervention. J. Pharmacol. Exp. Ther. 304, 1–7.

Liu Y., Liu J., Tetzlaff W., Paty D. W. and Cynader M. S. (2006) Biliverdin reductase, a major physiologic cytoprotectant, suppresses experimental autoimmune encephalomyelitis. Free Radic. Biol. Med. 40, 960–967.

Mandel S. G. E., Riederer P., Amariglio N., Jacob-Hirsch J., Rechavi G. and Youdim M. B. (2005) Gene expression profiling of sporadic Parkinson's disease substantia nigra pars compacta reveals impairment of ubiquitin-proteasome subunits, SKP1A, aldehyde dehydrogenase, and chaperone HSC-70. Ann. NY Acad. Sci. 1053, 356–375.

Mayeux R. (2003) Epidemiology of neurodegeneration. Annu. Rev. Neurosci. 26, 81–104.

McGeer P. L. and McGeer E. G. (1998) Glial cell reactions in neurodegenerative diseases: pathophysiology and therapeutic interventions. Alzheimer Dis. Assoc. Disord. 12(Suppl. 2), S1–S6.

McGeer P. L. and McGeer E. G. (2004) Inflammation and neurodegeneration in Parkinson's disease. Parkinsonism Relat. Disord. 10(Suppl. 1), S3–S7.

McLaughlin P., Zhou Y., Ma T., Liu J., Zhang W., Hong J. S., Kovacs M. and Zhang J. (2006) Proteomic analysis of microglial contribution to mouse strain-dependent dopaminergic neurotoxicity. Glia 53, 567–582.

Meini A., Garcia J. B., Pessina G. P., Aldinucci C., Frosini M. and Palmi M. (2006) Role of intracellular Ca2+ and calmodulin/MAP kinase kinase/extracellular signal-regulated protein kinase signalling pathway in the mitogenic and antimitogenic effect of nitric oxide in glia- and neurone-derived cell lines. Eur. J. Neurosci. 23, 1690–1700.

Mirza B. H. H., Thomsen P. and Moos T. (2000) The absence of reactive astrocytosis is indicative of a unique inflammatory process in Parkinson's disease. Neuroscience 95, 425–432.

Parente L. and Solito E. (2004) Annexin 1: more than an anti-phospholipase protein. Inflamm. Res. 53, 125–132.

Przedborski S., Chen Q., Vila M., Giasson B. I., Djaldatti R., Vukosavic S., Souza J. M., Jackson-Lewis V., Lee V. M. and Ischiropoulos H. (2001) Oxidative post-translational modification of alpha-synuclein in the 1-methyl-4phenyl-1,2,3,6-tetrahydropyridine (MPTP) mouse model of Parkinson's disease. J. Neurochem. 76, 637–640.

Qin L., Wu X., Block M. L., Liu Y., Breese G. R., Hong J. S., Knapp D. J. and Crews F. T. (2007) Systemic LPS causes chronic neuroinflammation and progressive neurodegeneration. Glia 55, 453–462.

Reynolds A. D., Banerjee R., Liu J., Gendelman H. E. and Mosley R. L. (2007) Neuroprotective activities of CD4+CD25+ regulatory T cells in an animal model of Parkinson's disease. J. Leukoc. Biol. 82, 1083–1094.

Singleton A. B., Farrer M., Johnson J. *et al.* (2003) alpha-Synuclein locus triplication causes Parkinson's disease. Science 302, 841.

Souza J. M., Giasson B. I., Chen Q., Lee V. M. and Ischiropoulos H. (2000) Dityrosine cross-linking promotes formation of stable alpha-synuclein polymers. Implication of nitrative and oxidative stress in the pathogenesis of neurodegenerative synucleinopathies. J. Biol. Chem. 275, 18344–18349.

Spira P. J., Sharpe D. M., Halliday G., Cavanagh J. and Nicholson G. A. (2001) Clinical and pathological features of a Parkinsonian syndrome in a family with an Ala53Thr alpha-synuclein mutation. Ann. Neurol. 49, 313–319.

Spillantini M. G., Schmidt M. L., Lee V. M., Trojanowski J. Q., Jakes R. and Goedert M. (1997) Alpha-synuclein in Lewy bodies. Nature 388, 839–840.

Sriram K., Matheson J. M., Benkovic S. A., Miller D. B., Luster M. I. and O'Callaghan J. P. (2002) Mice deficient in TNF receptors are protected against dopaminergic neurotoxicity: implications for Parkinson's disease. FASEB J. 16, 1474–1476.

Sung J. Y., Park S. M., Lee C. H., Um J. W., Lee H. J., Kim J., Oh Y. J., Lee S. T., Paik S. R. and Chung K. C. (2005) Proteolytic cleavage of extracellular secreted α-synuclein via matrix metalloproteinases. J. Biol. Chem. 280, 25216–25224.

Taki J., Nakajima K., Hwang E. H., Matsunari I., Komai K., Yoshita M., Sakajiri K. and Tonami N. (2000) Peripheral sympathetic dysfunction in patients with Parkinson's disease without autonomic failure is heart selective and disease specific, taki@med.kanazawa-u.ac.jp. Eur. J. Nucl. Med. 27, 566–573.

Tanner C. M. (1992) Occupational and environmental causes of parkinsonism. Occup. Med. 7, 503–513.

Teismann P. and Ferger B. (2001) Inhibition of the cyclooxygenase isoenzymes COX-1 and COX-2 provide neuroprotection in the MPTP-mouse model of Parkinson's disease. Synapse 39, 167–174.

Teismann P., Tieu K., Choi D. K., Wu D. C., Naini A., Hunot S., Vila M., Jackson-Lewis V. and Przedborski S. (2003) Cyclooxygenase-2 is instrumental in Parkinson's disease neurodegeneration. Proc. Natl Acad. Sci. USA 100, 5473–5478.

Thomas M. P., Chartrand K., Reynolds A., Vitvitsky V., Banerjee R. and Gendelman H. E. (2007) Ion channel blockade at-

tenuates aggregated alpha synuclein induction of microglial reactive oxygen species: relevance for the pathogenesis of Parkinson's disease. J. Neurochem. 100, 503–519.

Vijitruth R., Liu M., Choi D. Y., Nguyen X. V., Hunter R. L. and Bing G. (2006) Cyclooxygenase-2 mediates microglial activation and secondary dopaminergic cell death in the mouse MPTP model of Parkinson's disease. J. Neuroinflammation 3, 6.

Vilhardt F. (2005) Microglia: phagocyte and glia cell. Int. J. Biochem. Cell Biol. 37, 17–21.

Vuadens F., Rufer N., Kress A., Corthesy P., Schneider P. and Tissot J. D. (2004) Identification of swiprosin 1 in human lymphocytes. Proteomics 4, 2216–2220.

Walther M., Kuklinski S., Pesheva P., Guntinas-Lichius O., Angelov D. N., Neiss W. F., Asou H. and Probstmeier R. (2000) Galectin-3 is upregulated in microglial cells in response to ischemic brain lesions, but not to facial nerve axotomy. J. Neurosci. Res. 61, 430–435.

Wang X., Chen S., Ma G., Ye M. and Lu G. (2005) Involvement of proinflammatory factors, apoptosis, caspase-3 activation and Ca2+ disturbance in microglia activation-mediated dopaminergic cell degeneration. Mech. Ageing Dev. 126, 1241–1254.

Wersinger C. and Sidhu A. (2006) An inflammatory pathomechanism for Parkinson's disease? Curr. Med. Chem. 13, 591–602.

Wu D. C., Jackson-Lewis V., Vila M., Tieu K., Teismann P., Vadseth C., Choi D. K., Ischiropoulos H. and Przedborski S. (2002) Blockade of microglial activation is neuroprotective in the 1-methyl-4-phenyl-1,2,3,6-tetrahydropyridine mouse model of Parkinson disease. J. Neurosci. 22, 1763–1771.

Wu D. C., Teismann P., Tieu K., Vila M., Jackson-Lewis V., Ischiropoulos H. and Przedborski S. (2003) NADPH oxidase mediates oxidative stress in the 1-methyl-4-phenyl-1,2,3,6-tetrahydropyridine model of Parkinson's disease. Proc. Natl Acad. Sci. USA 100, 6145–6150.

Zarranz J. J., Alegre J., Gomez-Esteban J. C. *et al.* (2004) The new mutation, E46K, of alpha-synuclein causes Parkinson and Lewy body dementia. Ann. Neurol. 55, 164–173.

Zbarsky V., Datla K. P., Parkar S., Rai D. K., Aruoma O. I. and Dexter D. T. (2005) Neuroprotective properties of the natural phenolic antioxidants curcumin and naringenin but not quercetin and fisetin in a 6-OHDA model of Parkinson's disease. Free Radic. Res. 39, 1119–1125.

Zhang W., Wang T., Pei Z., Miller D. S., Wu X., Block M. L., Wilson B., Zhou Y., Hong J. S. and Zhang J. (2005) Aggregated alpha-synuclein activates microglia: a process leading to disease progression in Parkinson's disease. FASEB J. 19, 533–542.

Zhou Y., Wang Y., Kovacs M., Jin J. and Zhang J. (2005) Microglial activation induced by neurodegeneration: a proteomic analysis. Mol. Cell Proteomics 4, 1471–1479.